Available online at www.sciencedirect.com

jmr&t
Journal of Materials Research and Technology

journal homepage: www.elsevier.com/locate/jmrt

Original Article

A review of impact resistant biological and bioinspired materials and structures

Benjamin S. Lazarus [a,*], *Audrey Velasco-Hogan* [a], *Teresa Gómez-del Río* [a,c], *Marc A. Meyers* [a,b,d], *Iwona Jasiuk* [e]

[a] *Materials Science and Engineering Program, U. of California, San Diego, USA*
[b] *Mechanical and Aerospace Engineering Department, U. of California, San Diego, USA*
[c] *DIMME, Durability and Mechanical Integrity of Structural Materials, U. Rey Juan Carlos, Spain*
[d] *Nanoengineering Department, U. of California, San Diego, USA*
[e] *Mechanical Science and Engineering Department, U. of Illinois at Urbana-Champaign, USA*

ARTICLE INFO

Article history:
Received 5 June 2020
Accepted 20 October 2020
Available online 31 October 2020

Keywords:
Impact resistance
Biological materials
Bioinspiration
Structural design motifs
Hierarchical materials
Natural composite materials

ABSTRACT

Biological systems must have the capability to withstand impacts generated during collisions due to combat and defense. Thus, evolution has created complex materials' architectures at various length scales that are capable of withstanding repeated, low-to-medium-velocity impacts (up to 50 m/s). In this paper, we review impact resistant biological systems with a focus on their recurrent structural design elements, material properties, and energy absorbing mechanisms. We classify these impact resistant structures at the micro- and meso-scales into layered, gradient, tubular, sandwich, and sutured and show how they construct global hierarchical, composite, porous, and interfacial architectures. Additionally, we review how these individual structures and their design parameters can provide a tailored response. We conclude with a future outlook and discussion of their potential for impact resistant bioinspired designs.

1. Introduction

The impact between two bodies can initiate a cascade of damage events with dire consequences. This sequence depends on a number of structural factors as well as the velocity of impact. The damage is determined by the energy that is delivered to the participating bodies. This energy is expressed by the first law of thermodynamics as:

$$dE = \delta q - \delta W$$

where E is the internal energy, W is the work done by the system on the environment, and q is the heat transferred to the system from the environment. Neglecting the heat transfer effect in dynamic events:

$$dE = \delta W$$

The dominant internal energy component is considered to be the kinetic energy. In a very simplified manner, the work can be expressed as $F\Delta l$, where Δl is the distance over which the force F operates

* *Corresponding author.*
E-mail address: bslazaru@eng.ucsd.edu (B.S. Lazarus).
https://doi.org/10.1016/j.jmrt.2020.10.062

$$\frac{1}{2}mv^2 = F\Delta l$$

Thus, if the velocity doubles the force quadruples, for the same Δl. In real impact situations F is not constant but undergoes oscillations that depend on a number of structural and wave propagation effects. This is one of the aspects that distinguishes quasi-static from dynamic deformations. In quasi-static deformation the body is in static equilibrium, whereas in dynamic deformation, elastic and plastic waves propagate and the stresses experienced at any Lagrangian point are determined by the passage of these pulses.

The realm of impact is extremely broad and encompasses velocities as high as tens of thousands to few meters per second. In space, these can reach levels of 50 km/s. On earth, explosives, two-stage gas guns, lasers, and electromagnetic accelerators can launch projectiles at velocities in the range of 5–15 km/s. Ballistic impact by rifle and other projectiles occurs in the range of 200–1200 m/s. A baseball hurled by a professional, and impacted by a bat, can reach a velocity of 500 m/s. This is apparently also the maximum velocity of a stone thrown by a human. Arrow velocities range from 50 to 100 m/s. In a Hopkinson bar, a favorite instrument for dynamic testing, the striker hits the incident bar at a velocity of approximately 10 m/s.

Biological materials are only designed to resist the lower range of these velocities. The velocity of the mantis shrimp club reaches 23 m/s [1], and this might be the highest velocity recorded in the biological domain. Rams have impact velocities of around 5.5 m/s [2]. Sea otters drive bivalve shells against their chest or emergent rocks at a velocity of approximately 1–2 m/s [3]. Chimpanzees use stones to break nuts and hard-shelled fruits, and so do Capuchin monkeys in Brazil. Macaques in Southern Thailand use rocks to break shells. A woodpecker's beak hits the target at ~7 m/s [4]. A galloping horse's hoof impacts the ground at ~8 m/s [5].

The structural response of biological materials has been intensively studied over the past 50 years, with the works of Currey [6,7] and Vincent [8,9] representing the seminal contributions and approaches. Wegst and Ashby [10] developed elucidative performance diagrams for structural materials in terms of strength, elastic modulus, toughness, density, and other properties. These plots provide a highly useful ranking of and comparison among materials and have been used globally. More recently, comprehensive reviews by Meyers et al. [11] and Chen et al. [12], and more specific contributions on collagen [13,14] and keratin [15] have covered a broad range of performances, which are also reviewed by Meyers and Chen [16]. These studies led to the proposition that biological materials have common structural design elements which can be analytically expressed and quantified. They are found across species and are due, in many cases, to convergent evolution processes [17].

These studies have one limiting characteristic. Although strain rates are varied and recognized to have a significant effect on the deformation and failure processes, the regime explored can be classified as quasi-static. The present contribution represents a departure of these works in that deformations occur at strain rates that are characteristic of impacts.

Impact events can be divided into three types: (i) lower velocity impact (<2 m/s) where many problems fall into the area of structural dynamics; local indentations or penetrations are strongly coupled to the overall deformation of the structure; (ii) high velocity impact; and (iii) hypervelocity impact [18]. Low velocity impact is defined as an impact event where the time for the projectile in contact with the material exceeds the period of the lowest vibrational mode. In a low-velocity impact event, the boundary conditions of the structural component are required to accurately describe the impact response. As the striking velocity increases (between 0.5 and 1.5 km/s) into the high velocity impact (ballistic or blast impact) regime, the local material behavior in the impacted zone governs the impact response of the structure [18,19]; a wave description of the phenomenon is required and the influences of the velocity, geometry, material constitution, strain rate, localized plastic flow, and failure are manifested at various stages of the impact process. Still, further increases in impact velocity (starting at 2–3 km/s) result in a hyper-velocity impact event. The locally impacted material gradually behaves like a fluid and very high stresses are induced [20] by the shock waves whose propagation is governed by the Rankine–Hugoniot relations.

2. Classification of biological architectures and properties

Biological materials have developed, through evolution, a cornucopia of strategies to resist impact by minimizing damage. We will evaluate them here, inspired by the structural design elements proposed by Naleway et al. [17] but modifying them for impact. This is a framework which enables an evaluation of the mechanisms used by different organisms. The complex mechanical behavior of structural biological materials in the dynamic regime will be systematized through the proposal of this framework.

2.1. *General features of biological materials that affect impact resistance*

All biological materials, including impact resistant materials, have the following characteristics:

- **Hierarchical:** discrete structural elements identified across several length scales (nano, micro, meso, macro) that work synergistically to enhance the overall mechanical properties of the structure. All biological materials are hierarchical due to their self-assembly from the atomistic to macro-scale. Every other arrangement, whether a general feature or specific structure contributes to the hierarchical organization of biological materials.
- **Composite:** material made of two or more materials or phases, with distinct interfaces, having properties different from those of its constituents. Biological materials are composites typically made of a ceramic and a polymeric phase for mineralized systems or a crystalline and an amorphous phase for non-mineralized systems. The stiffer phase provides the necessary rigidity and strength while the soft phase imparts ductility. Often, biological composites outperform the simple composite nature of their constituent parts.

- **Porous:** gaps in solid material that are filled with air or fluid can exist across all length scales. All biological materials have some degree of porosity as various pore shapes and densities can be found throughout nature. Porous materials often increase the energy absorbing capabilities, with an added benefit of decreasing the overall weight.
- **Interfaces:** shared boundaries between two phases with different properties. Interfaces can arrest cracks, enhance flexibility, and contribute to the viscous response of materials during deformation. All biological materials have interfaces due to their composite nature. There is a vast array of arrangements and materials that are used to define these interfaces.

These components are found across nature and play a significant role in a material's impact resistance. The arrangement and magnitude of these features are also significant factors in a material's response to dynamic loading. In parallel, all biological materials exhibit viscoelastic and/or viscoplastic behaviors. This is due to the inherent response of their polymeric constituents during loading.

- **Viscoelastic**: material property exhibiting both viscous and elastic responses with time-dependent stress and strain. The damping of the pulses is an important characteristic of impact-resisting materials.
- **Viscoplastic**: material properties that involve time-dependent permanent deformations, including sliding, delamination, and microcracking. These mechanisms dissipate energy.

The time dependence of a material's response to loading is important during impact. This inelastic behavior is a result of the polymeric constituents found in biological materials (collagen, keratin, cellulose, hemi-cellulose, lignin, and chitin) which ultimately determines deformation mechanisms and their capacity to absorb and dissipate energy under dynamic conditions. This material behavior can be expressed by the time constant in stress relaxation and by the ratio of loss to storage moduli (tan (delta)) in the regime of interest. The features identified in this section are found across all biological materials.

2.2. *Specific architectures found in impact resistant biological materials*

Additionally, many impact resistant biological systems have developed specific impact resistant structural elements typically found on the micro- and meso-scale which include:

- **Layered:** laminate layers with distinct interfaces which serve as crack dissipators. Fiber orientations often change from layer to layer, either in plane (laminated structures) or out-of-plane (Bouligand structures).
- **Gradient:** a gradual change in a material property (e.g., modulus, density), architecture (e.g., porosity), and/or composition.
- **Tubular:** hollow channels typically aligned along a given axis.
- **Sandwich:** two stiff layers separated by a softer, porous layer allowing for a lightweight yet stiff, strong, and energy absorbent material.
- **Sutured:** an interlocking interface connecting two neighboring components.

These elements are found in a variety of biological systems that experience impact and are often used in conjunction with each other, leading to impressive properties under dynamic loading. While these structures act as the building blocks for hierarchical, impact resistant structures, tests using computer simulations, 3D printing, and composite prepregs have allowed researchers to probe the function of these architectures as independent designs. Many studies have found that even as the sole design component, each of these arrangements can improve the impact resistance of a material.

First, the characteristics of these impact resistant structural and material elements are presented by discussing the most important impact resistant biological materials and classifying them into groups based on their material constituents. Properties related to the impact resistance of biological materials will be evaluated using this framework in Section 3.

Then, we present the essential features of each structural design element, as defined by Naleway et al. [16], and take examples from nature where they are used to improve impact resistance (Section 4 and 5).

Since the ultimate objective of this study is to aid in the development of bioinspired designs, we also include a brief section (Section 6) outlining evolving applications, current engineering approaches to impact resistance, and (Section 8) possible future directions.

While the main focus of this review is on structural design motifs, it is important to clarify that the inelastic behavior or time-dependent behavior of biological materials, which is the result of their polymeric constituents, is an important contributor for impact resistance. In this review we will address the strain-rate dependence and sensitivity of biological systems and focus on viscoelasticity/viscoplasticity to describe their inelastic behavior.

3. Impact resistant biological systems

A defining feature of biological materials is their hierarchical structure, that is, an arrangement that incorporates geometries across multiple length scales. Since biological materials self-assemble from the atomistic level, they are capable of controlling the formation of intricate structures at each length scale. In this vein, natural systems often integrate several different impact resistant strategies in one material. The result is a complex combination of nano-to macro-structural features that work synergistically to absorb impacts, dissipate energy, and constrain damage to prevent catastrophic failure.

This section will highlight nature's most successful impact resistant materials and will identify several trends that are observed in representative systems. We group these materials into the following categories: cellulose, hemi-cellulose, and lignin systems (fruits, nuts, and wood), keratinized systems

(horns, hooves, pangolin scales), collagenous systems (tendons, ligaments, cartilage), and mineralized systems (bone, skulls, turtle carapace, and marine systems).

3.1. *Cellulose, hemi-cellulose, and lignin systems*

Many nuts and fruits need to be able to endure the natural process of falling to the ground and seed dispersal mechanisms which can involve significant impact forces. Tree trunks are exposed to dynamic loading during extreme natural events such as avalanches or hurricanes. These systems are also subjected to impacts from animals and even from other trees falling. This section focuses on the dynamic loading conditions and the energy absorbing mechanisms of cellulose, hemi-cellulose, and lignin based systems.

3.1.1. *Nuts and fruits*

Pomelos have developed a protective exterior that has three distinct layers: a compact layer of external cells (exocarp), a thick spongy middle layer (mesocarp), and a dense layer adjacent to the fruit's pulp termed the endocarp. This layered system is conventionally referred to as a sandwich structure. The dense endocarp and exocarp are tough and prevent puncture while the highly porous, fluid-filled, mesocarp can collapse elastically absorbing strain energy. The mesocarp can reach a porosity of up to 80% and only begins to densify after 55% strain [21].

Similarly, coconuts have a three-layered sandwich structure, with a firm exterior and internal layer with a soft mesocarp in between [21]. The coconut shell is highly hierarchical, having hollow channels (~200 μm diameter) surrounded by hollow fibers (~15 μm diameter) whose walls are composed of an intercellular ladder structure (with gaps on the scale of 1–10 μm) [22]. As the coconut ages, it becomes more porous and has higher strength and fracture toughness [22]. The microstructures of old and young coconuts are shown in Fig. 1. The porous nature of the coconut mesocarp has also been shown to trap, blunt, and deflect cracks, forcing them to take circuitous paths [22]. In older coconuts, these effects are magnified as can be seen in Fig. 2A, where cracks

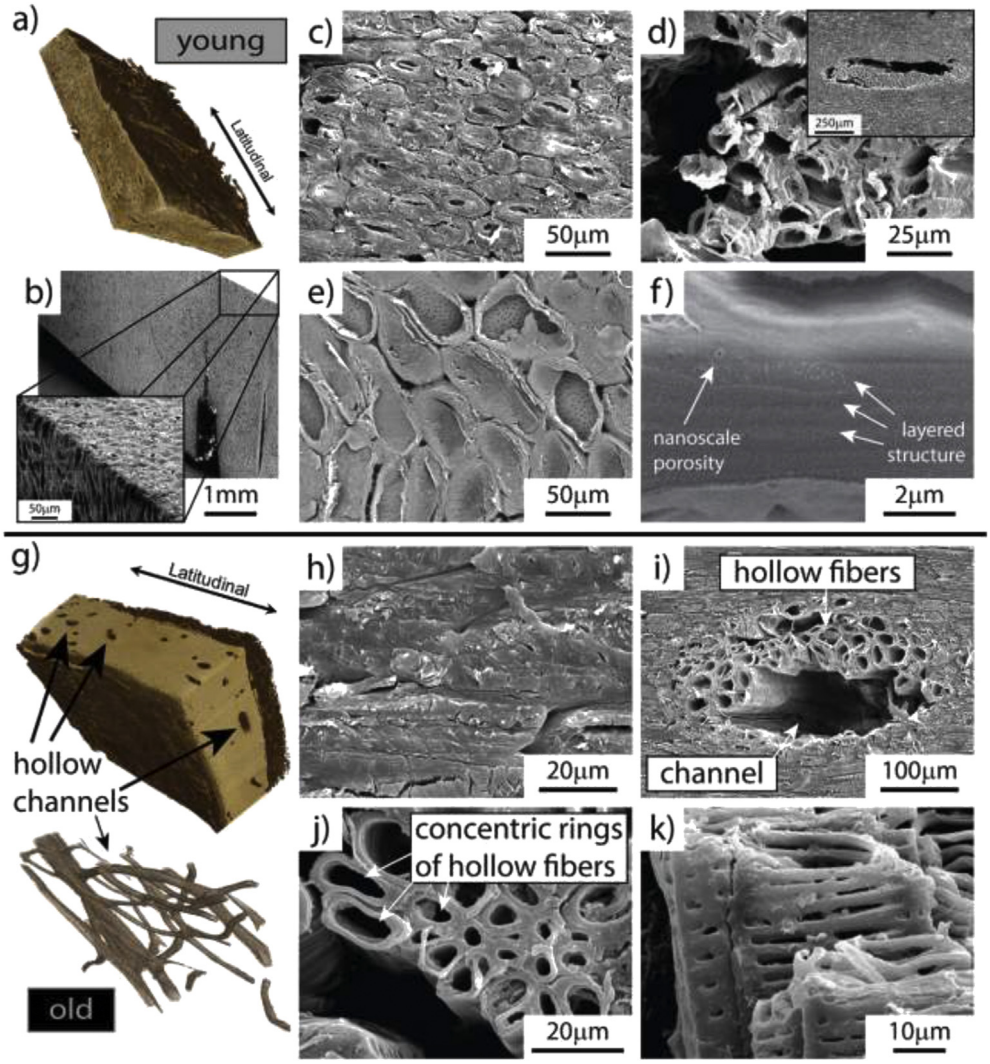

Fig. 1 – Structural comparison of young and old coconuts. Coconuts develop a porous hierarchy composed of hollow channels, surrounded by hollow fibers with ladder structured walls, and nanopores embedded in the lamellar arrangement of the coconut shell [22]. Adapted with permission [22] Copyright 2017, Elsevier.

formed in old coconuts (i,ii) are jagged and tortuous compared to the relatively straight cracks (iii,iv) in young coconuts. This leads to improved strength as well as crack initiation and growth toughness in older coconuts (v-viii) [22]. Further, individual fibers and fiber bundles in the coconut mesocarp are capable of enduring strains up to 40% before experiencing benign failure [21]. The porosity and fiber ductility of the mesocarp allow the coconut to sustain significant deformation without failure.

Fig. 2B shows the typical stress–strain curve for the foam sandwich structures found in coconuts and pomelos. In the first region of the curve, the stress and strain rise to the necessary threshold to begin deforming the porous central layer of the material. Once this stress level has been achieved, it remains relatively constant while the foam layer begins to compact. This process of pore collapse absorbs significant amounts of energy, even at higher strain rates. Damage begins to occur in the rest of the material only after the pores have been compacted. This structure is not only impact resistant due to its high strain endurance, but also because it spreads the impact throughout the porous network as it collapses. This is important for pomelos and coconuts which can resist impact energies up to 1.5 kJ [21].

3.1.2. *Trunks and stems*

Many woods can be conceptualized as closed cell foams with a rigid outer layer (bark) and a stiff compact core creating a porous sandwich structure. Different species have different porous arrangements which can be seen in Fig. 2C (i-iv). Matsushita et al. [23] examined eight different wood species under impact conditions and concluded that the banded nature of the woods affected their impact strength. While pores sometimes act as crack arresters, they can also act as flaws that initiate cracks and delamination. Fig. 2C (viii) shows microcomputed tomography images of white ash after impact. Near the impact center, delamination initiates at pores which is outlined in red. When pores are packed close together in ring or semi-ring porous arrangements, this effect is magnified leading to rapid catastrophic failure at the porous bands. Farther from the impact zone compressed pores and cracks that are arrested at pore interfaces are outlined in yellow and black, respectively. Several of the species that were tested also contained arrangements of aggregated ray cells. These cells are more rigid than the surrounding tissue and when grouped into large bundles divide the pores into enclosed sections. Matsushita et al. [23] determined that these bundles localize the damage zone of the material, so that only small areas of the porous structure are affected by the impact. Fig. 2C (v,vi) shows how the rigid rays can confine cracks. In these instances, very little material contributes to the dissipation of impact energy. Further, these bundles compartmentalize crack deflection, resulting in straight smooth cracks unlike the rough cracks that meandered through the porous networks found in similar wood species without aggregated ray cell bundles (Fig. 2C (vii)).

Of the eight types of wood tested, African mahogany exhibited the best impact resistance. It dissipated energy via fiber bending and pullout, a mechanism observed in a number of other biological systems [24] as well as in engineered composites [25]. After impact, entire tracheid fibers would be bent, the ends of which showed evidence of cell wall delamination and helical unwinding. These processes significantly delocalize damage and absorb energy without causing catastrophic failure. Less impact resistant species, like white oak, did not disperse the load throughout the entire material and instead simply fractured across fibers near the impact zone. Other species, such as Red alder, dissipated energy through fiber bending before rupturing under low force. Fig. 2C (ix) shows the force displacement curves of these three species alongside SEM images that illustrate these deformation mechanisms. The most impact resistant of the species, African mahogany, had an intermediate force displacement curve, enduring larger displacements than White oak while also exhibiting larger peak forces than Red alder. Matsushita et al. [23] contends that wood can be viewed as a fiber reinforced composite, where adhesion between the fibers in the wood and the surrounding matrix is key to understanding the impact resistance. Adhesion plays a particularly important role at higher strain rates, when the viscous response of the wood is minimized and shear stress between the fibers and the surrounding matrix builds rapidly.

3.2. *Keratinized systems*

Keratin is a highly prevalent protein in nature, found in the integument of a variety of animals. Keratinous materials serve a wide range of functions such as insulation (i.e., hair and wool), filtration (i.e., whale baleen), and flight (i.e., feathers). Additionally, one of the most common uses of keratinous materials in nature is for impact-resistant applications. The hoof walls of many ungulates such as horses, bovines, and donkeys are composed almost entirely of keratin. The same is true for the horns of the bighorn sheep, yaks, and rhinoceros. These body parts experience repeated impacts over the course of an animal's life and since keratin is often embedded in dead cells that do not self-repair, these durable structures are prime candidates for biomimetic materials. The outer-most layers of many defensive biological systems, such as turtle shells and armadillo armor, are composed of keratin scutes. However, the primary structural components of these systems are the subdermal bony layers, so they will be discussed in the next section. Pangolins, on the other hand, have a dermal armor composed solely of overlapping keratin scales that provide protection from predators like lions [26]. Important keratinous structures will be examined in this section.

3.2.1. *Hooves and horns*

The hooves of horses suffer repeated high impacts with a deceleration of ~43 g [5]. Horse hooves are composed of keratin and, like all keratinous materials, have mechanical properties that are highly dependent on hydration. The hoof has two hydration gradients, (1) distal to proximal and (2) interior to exterior. These hydration gradients originate at the living tissue adjacent to the hoof which supplies moisture to the dead keratin cells. The exposed surfaces of the hoof release moisture and dry out more quickly than the internal layers. These variations in hydration lead to a significant gradient in the mechanical properties of the hoof, since dry keratin is stiffer and less tough than hydrated keratin [27]. This stiffness gradient is further enhanced by a slow decrease

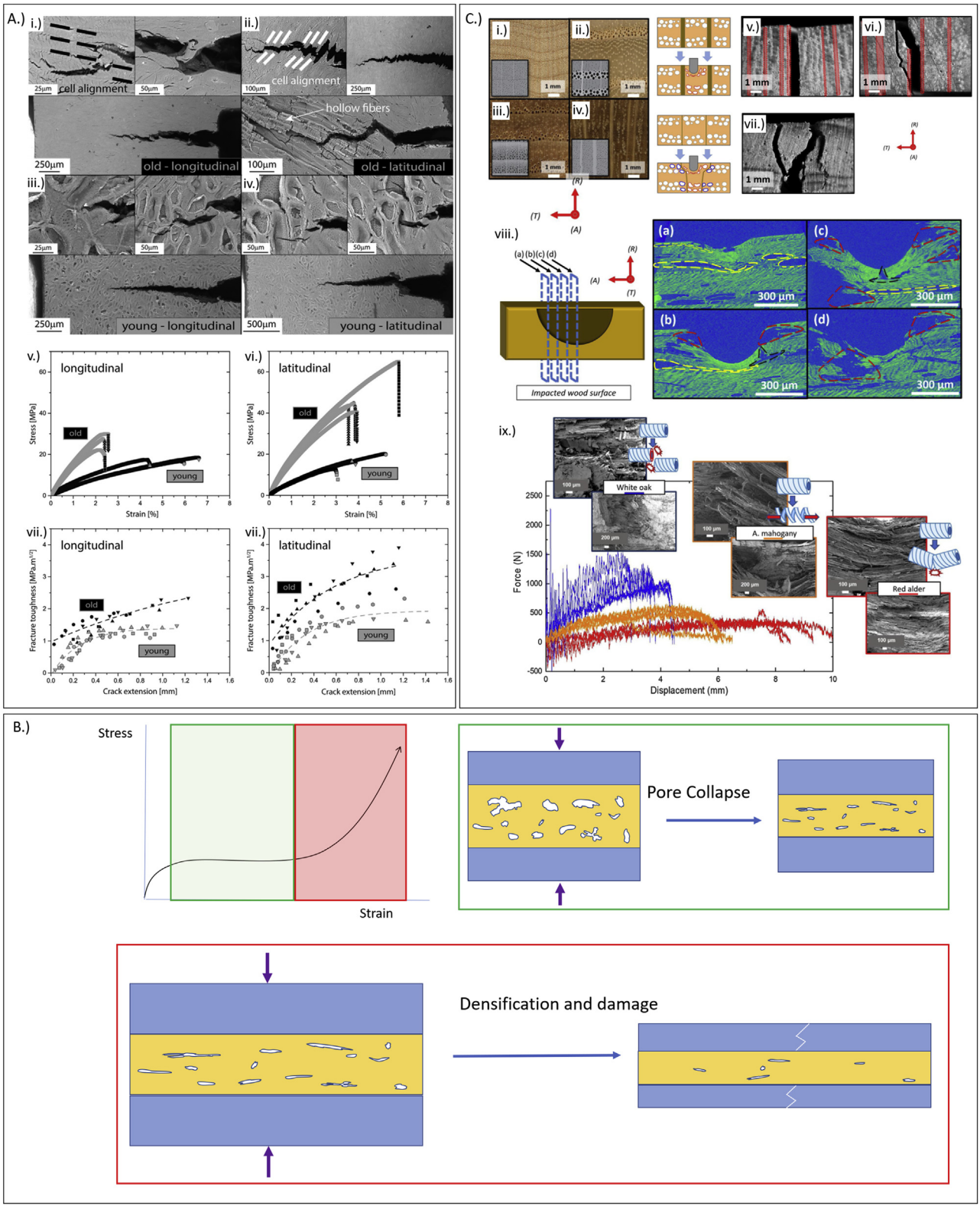

Fig. 2 – Impact results on cellulose, hemi-cellulose, and lignin based systems. A) (i-iv) Fracture patterns in old and young coconuts loaded in tension in the longitudinal and latitudinal directions. (v & vi) Stress strain curves obtain from tensile testing and (vii-ix) K_j (resistance) R-curves for coconut fracture tests performed under three-point bending conditions [22]. B) Typical stress strain curve for biological sandwich structures; there is an initial linear elastic response from the material, followed by the green region of the stress–strain curve where the foam's pores collapse, allowing for high strain endurance and energy absorption, until finally in the red region of the stress–strain curve the foam layer has densified and can no longer collapse anymore, resulting in plastic deformation and damage. C) Wood structure and deformation under impact. (i-

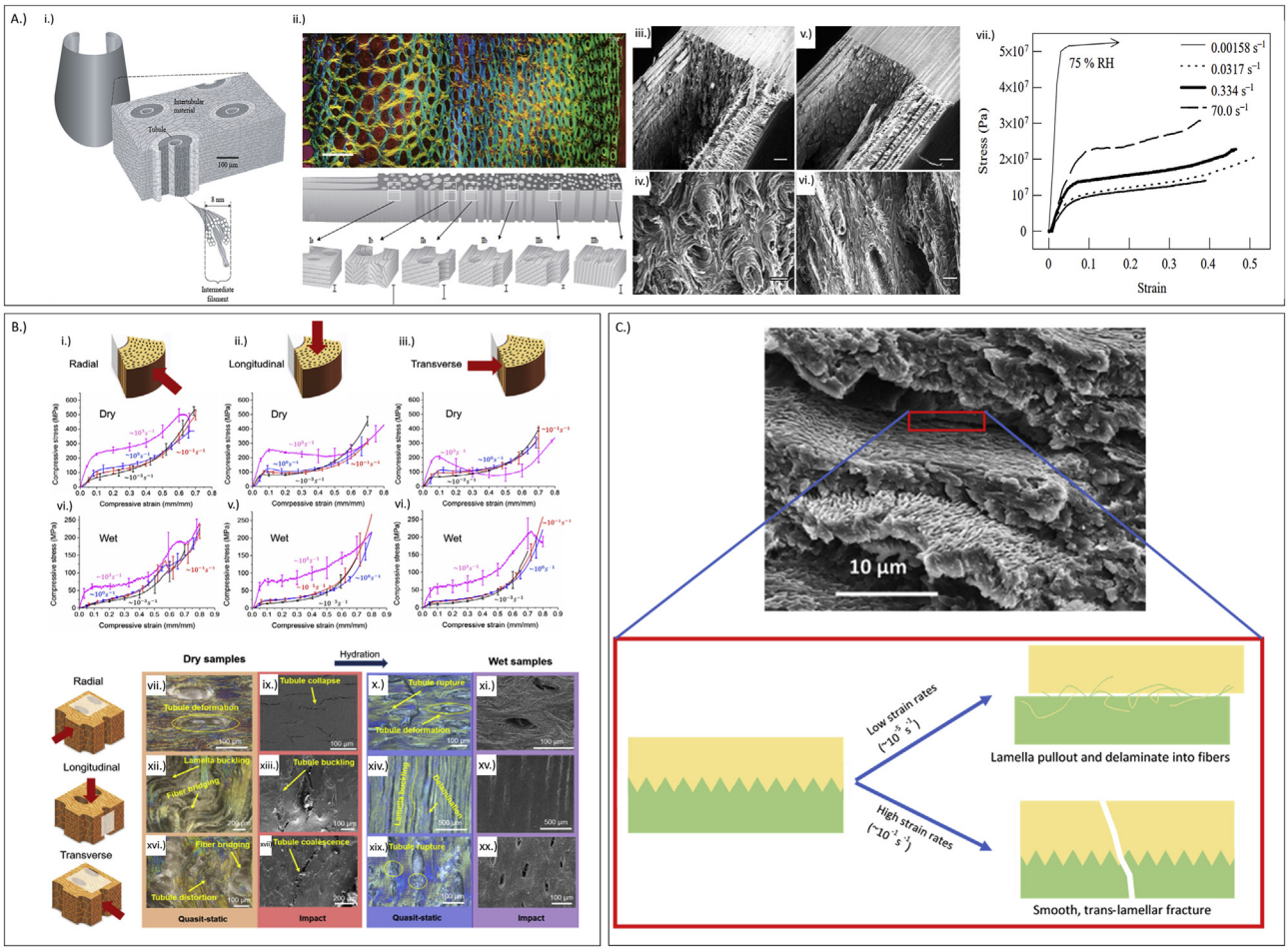

Fig. 3 – Keratinous systems such as hooves, horns, and pangolin scales exhibit common impact resistant structures. A) (i) Horse hooves have reinforced tubular elements embedded in a lamellar intertubular matrix [28]. (ii) There are several gradients in these tubular structures which vary in shape, size and density through the thickness of the hoof wall. All of these features are composed of dead cells that are embedded with keratin intermediate filaments. These cells form layers whose arrangement can be seen in the bottom of Fig. 3A (ii) [34]. (iii, iv) The fracture pattern of horse hooves under tension at low strain rates alongside (v,vi) the fracture pattern of horse hooves at high strain rates. (vii) The stress-strain curve of the horse hoof at different strain rates [30]. B) (i-vi) Stress-strain curves of bighorn sheep horn under compression in three different directions. Each orientation was compressed at three different strain rates under wet and dry conditions. (vii-xx) Optical and SEM images show the different deformation mechanisms of the horn under varying loading conditions, hydration levels, and orientations [41]. C) The sutured pangolin lamellae have different deformation mechanisms at high and low strain rates. At low strain rates, lamella pullout and delaminate while at high strain rates, there is a smooth fracture across the interface. These mechanisms are shown in the schematic [26]. Adapted with permission [28] Copyright 1999, Company of Biologists. Adapted with permission [34]. Adapted with permission [30]. Adapted with permission [41] Copyright 2017, Acta Materialia. Adapted with permission [26], Copyright 2016, Elsevier.

in keratin intermediate filament density from the exterior of the hoof to the interior [28]. This gradient structure allows the load-bearing keratin of the hoof wall to dissipate energy to the skeletal structure while also cushioning sensitive tissue at the hoof interior [29]. The hard, exterior surfaces of the hoof are firm and puncture resistant. Since the hoof wall becomes tougher towards the interior, cracks that are traveling inward will often be blunted and can more easily be redirected [30].

iv) Different arrangements of pores and aggregate rays and (v-vii) the fracture patterns of representative wood samples under impact. (viii) Micro-computed tomography images of wood after impact at 0.4 mm, 0.3 mm, 0.2 mm, and 0.1 mm respectively from the impact center. (ix) Force displacement curves of three different types of wood, with images showing their deformation mechanism [23]. Adapted with permission [22] Copyright 2017, Elsevier. Adapted with permission [23] Copyright 2019, Elsevier.

Similar hydration gradients can be found in other keratin systems such as steer horn sheathes, where the hydrated base of the horn wall is more flexible, increasing bending toughness under impact [31].

Additionally, there exist gradients in tubule shape, size, and density found in the hoof wall. The hollow tubules in the hoof are approximately 40 μm in diameter and are surrounded by a rigid cortex of dense keratin as seen in Fig. 3A (i) [32]. Towards the edge of the hoof wall the volume fraction of tubules increases and the shape of the tubules becomes more elliptical and smaller as shown in Fig. 3A (ii) [27,33]. These gradients in tubule shape, size, and density serve multiple functions. The denser tubules provide more reinforcement along the outside of the hoof, enhancing the stiffness gradient, and deflecting cracks away from the living tissue at the interior of the hoof. The change in tubule shape is thought to increase the moment of inertia as a response to the significant bending stresses found at the edges of the hoof during impacts [27,29]. Hopkinson bar impact testing on hoof showed minimal cracking in the tubular region, suggesting that the tubules deflect cracks. Further, the reinforced tubules prevented the shear banding that is evident in similar tests on horns. Compression tests along the tubule axis showed that the tubules buckle and crack to dissipate energy but are able to completely recover their shape at strains up to 30%, indicative of the viscoelastic behavior of the keratin [32].

While horse hoof walls have both a tubular and gradient character, they also have a tri-laminar ply structure that varies in orientation through the hoof [30]. At the nanometer level, the keratin in horse hooves is arranged into intermediate filaments (IFs) that are approximately 7 nm in diameter. These filaments fill cells which interlock with wavy, suture like surfaces and then align themselves into layers with weak interfaces in between them [34,35]. This hierarchical structure is depicted in Fig. 3A (i). As cracks propagate within the hoof wall, they get caught in these sacrificial layers which deflect them away from the living tissue at the hoof's interior. In fact, notched tensile testing revealed that it is nearly impossible to propagate a crack through the hoof in any direction other than between the aligned IFs, regardless of the orientation of the notch [36]. Fig. 3A (ii) shows the orientation of the IFs, with filaments oriented radially in the hoof appearing yellow, axially oriented filaments appearing blue, and filaments perpendicular to the hoof section appearing purple.

High strain rate tensile tests confirmed that in the central portion of the hoof wall, cracks had a strong tendency to travel along the intercellular, laminar planes (pictured at the bottom of Fig. 3A (ii)) similar to the quasi-static tensile tests, while in the inner and outer regions of the hoof, cracks traveled along tubule interfaces leading to delamination. The response of the hoof under impact is a prime example of how quasi-static tests can be useful for understanding a material under dynamic loading but do not always capture the full nature of a material's impact resistance. Fig. 3A (iii, iv) shows fracture patterns of the hoof at low strain rates compared to the fracture pattern of the hoof at high strain rates (v,vi). Impacted samples had smoother fractures and less tubule pullout but experienced the same regional preferences for the cracking direction. The viscoelastic nature of the hoof keratin has also been shown to increase the toughness of the hoof with increasing strain rate and lead to crack tip rounding. However, at higher strain rates smoother fracture patterns through cellular layers and less tubule pullout were observed, suggesting brittle failure for higher velocity impacts [30]. This is akin to what is observed in toucan beak keratin [37]. At higher strain rates, the hoof absorbed more energy and had a higher ultimate stress, as can be seen in Fig. 3A (vii). All of the lower curves are on samples that were kept fully hydrated and then left in ambient conditions for 24 hours. The upper curve labeled "75% RH" is a sample that was left in a 75% relative humidity environment until it equilibrated. The difference in the shape and maximum values of the stress–strain curves shows how hydration can drastically affect the properties of the hoof [30].

Lee et al. [38] performed drop tower tests on elk antler, steer horn, ram horn, armadillo carapace, and abalone and concluded that delamination was one of the dominant modes of energy dissipation in each material. They proposed that the large increase in surface area that occurs with delamination represents a highly effective mechanism of absorbing energy. The most impact resistant structure tested by Lee et al. [38] was the steer horn sheath in ambient hydration conditions, which exhibited a normalized failure impact strength of 99 kJ/m^2. This value was over eight times that of abalone and nearly twice the one for elk antler. Significant amounts of energy were dissipated by internal delamination within the horn samples during impact. Steer horn likely accomplishes this high impact strength with the wavy lamellar layers formed by keratinized cells in the sheath wall. These wavy layers resist the nucleation of new cracks and impede crack propagation. Further, the interfaces between the lamellae are characterized by labyrinth-like surfaces, which create large amounts of interlaminar friction during delamination [31].

Horns of other species, such as the yak and bighorn sheep, also possess impressive impact properties. The yak horn is a tapered, gradient structure that is narrow at the tip and gradually widens towards the base. It is composed of a keratin sheath around a bony core. The tip of the yak horn is older and denser and exhibits higher hardness, strength, and energy absorption under impact. Quasi-static compression tests revealed a multitude of failure mechanisms including densification under lateral tests and lamellar buckling, delamination, and fiber tearing in the keratin sheath when the samples were compressed axially. However, impact testing of the yak horn revealed a lower energy absorption and brittle failure at higher strain rates. This is counterintuitive, considering that the horn's primary role in nature is under impact. The authors [39] suggested that this may have been a result of ambient moisture levels that were not representative of the fresh yak horn. This example underscores the importance of hydration and the difficulties of comparing results between studies on biological samples when ambient conditions are not the same.

Bighorn sheep horns have a similar composition to yak horn but are spiraled rather than straight. This macroscale geometry makes the horn act as a loaded torsion spring which vibrates after impact to dissipate energy. The porous trabecular bone found in the core of the horn resists bending and absorbs a significant amount of strain energy during impact [40]. The keratin sheath of the horn has an intricate microstructure of tubules and cell lamellae which are oriented at a 30° angle to each other [41]. Similar to the hoof, there is a

porosity gradient through the hoof with a porosity of ~10% at the exterior of the keratin and 0% at interior. However, the tubules are oriented perpendicular to the loading direction, unlike hooves where tubules are parallel to the impact [42]. The lamellar cells are pancake shaped and filled with keratin fibers (intermediate filaments) that are in-plane with the flat surface of the cell. Fig 3B (i-iv) shows the response of horn samples in the wet and dry states under various loading conditions (different strain rates and orientations). Dry samples exhibited much larger stresses as water softens the keratin and makes it more compliant. However, dry samples were also much more anisotropic, performing noticeably better when compressed in the radial direction (the natural loading direction). This was true for impact and quasi-static tests. This anisotropy arises from the asymmetrical microstructure, although hydration can override these effects. Some of these microstructural effects can be visualized in Fig. 3B (vii-xx). When dynamic loading is applied along the radial direction (Fig. 3B(i)), the tubules oriented perpendicular to the impact direction collapse, absorbing significant amounts of energy. Impacts from other directions lead to shear banding, delamination, microcracking, buckling of the lamellae as well as tubule buckling but absorb less energy and recover less after impact [41]. Wet samples (xi, xv, xx) showed no obvious microstructural damage under impact, strengthening the claim that hydration can override microstructural effects. Similar to horse hooves, the bighorn sheep horn absorbed more energy and withstood larger stresses at higher strain rates. Much like yak horn, bighorn sheep horn properties are highly dependent on hydration, exhibiting brittle failure and anisotropy at low moisture levels. In the hydrated state, the horn is more isotropic, recovers its original length after dynamic loading at strains of up to 30%, and becomes much more ductile [41,43].

3.2.2. *Pangolin scales*

Fiber orientation has also been explored in pangolin scales where a crossed-fiber arrangement exists between crossed-lamellar structures which are interlocked with sutures. While each of these structures undoubtedly contributes to the mechanical properties of the scales, the crossed-fiber arrangement is unique compared to other keratinized systems. When torn, the pangolin scales fracture in a zig-zag manner unlike fingernails or feather rachis which have uniaxially oriented fibers and tear in smooth lines. In nature, systems like fingernails and feathers are typically subjected to predictable uniaxial stress, whereas the impact experienced by pangolin armor is unpredictable and can be multidirectional. With fibers crossed in multiple directions it is difficult for cracks to propagate through the lamellae. Failure of the scale at low strain rates typically requires fracturing or delaminating these crossed-fibers as the lamellae pull apart. At high strain rates, these mechanisms begin to break down and the lamellae do not have time to delaminate and deform. Instead they experience brittle failure with smooth fracture surfaces through lamellae [26]. These failure mechanisms and their strain rate dependence are illustrated in Fig. 3C.

3.3. *Collagenous structures*

Collagen is the most abundant protein in mammals, serving as a building block of most tissues with mechanical functions. Collagen has a hierarchical structure and a characteristic axial 67 nm periodicity seen in electron microscopy images [44,45]. Many tissues are made of collagen, including bone, tendon, ligament, muscle, intervertebral disc, intestine, cornea, and others [44,45]. Collagen provides strength in tension for soft tissues and flexibility, keeps the form, and serves as a framework for mineralization in hard tissues. Experimental studies on collagen report initially linear stress–strain curves and time-dependent recovery (i.e., viscoelastic behavior) [46,47].

3.3.1. *Tendons and ligaments*

The tendon has the highest content of collagen out of all collagenous tissues. Its function is to connect a muscle to the bone while ligament's purpose is to link bones together. Tendons and ligaments also facilitate motion and keep joint stability. They are subjected to uniaxial tensile loadings along their length. Thus, it is not surprising that their fibrous structures at different scales are all aligned in one direction. Their functions require that they are elastic and flexible but sufficiently stiff to transmit tensile forces and absorb large amounts of energy, such as in landing from a jump. This combination of properties is achieved by their hierarchical organization, which includes waviness at different scales and sliding of elements at different structural levels.

The hierarchical organization in tendon and ligament allows the distribution of stresses at each level of structure, minimizing stress concentrations, which could lead to failure and fracture. Such architecture is advantageous in handling dynamic and fatigue loadings. The stress–strain curve exhibits initial non-linear behavior due to fiber uncoiling, which can be extended with very little force, followed by a steeper, linear segment resulting from progressive straightening of the crimps. At normal physiological loads, the material response is at the initial non-linear toe region [45]. At very high strains, collagen fibers start to disassociate into subfibers, fibrils, and microfibrils, accompanied by yielding and irreversible damage. Tendons and ligaments have time- and history-dependent viscoelastic/viscoplastic properties, which are due to viscoelasticity of solid phase and water interaction with ground substance [45,48]. Tendons and ligaments are connected to bone, which is mineralized and thus has much higher stiffness. Those interfaces are again highly hierarchical, composite, and functionally graded to minimize stresses at the junctions [49].

3.3.2. *Cartilage*

Cartilage is a connective tissue that is present in three different forms (hyaline, fibrous, and elastic). Articular (also called hyaline) cartilage makes up the fetal skeleton, ribs, the wall of thorax, and the friction-reducing material at joints. Fibrous cartilage forms discs in spine which render it flexible, while elastic cartilage is found in nose, ears, and walls of thorax and larynx. Our interest is in articular cartilage, found at joints, which has impressive ability to absorb high loads [45,50].

Articular cartilage, when healthy, provides a smooth and low-friction surface for joints, excellent lubrication in combination with synovial fluid, cushioning, and it distributes applied forces to the underlying bone. Its excellent and multifunctional properties are due to its composite and hierarchical structure. Articular cartilage is a composite material consisting of 20–30 wt% of a solid phase (mainly collagen Type II and proteoglycans), with the rest being a fluid. The following structural scales can be identified in articular cartilage: (a) nanoscale – the dense extracellular matrix (ECM) consisting of water, collagen, proteoglycans and other organics, (b) microscale – the ECM and small percentage of cells, (c) mesoscale – the four zones: the tangential, intermediate, radiate, and calcified zones, and (d) macroscale – the functionally graded fluid-filled cartilage tissue [45,50,51].

In the tangent zone collagen fibers are aligned tangentially to the surface to resist shear stresses exerted by bone; in the intermediate zone fibrils are randomly arrayed and less densely packed; in the radiate zone fibrils are aligned normal to the underlying bone, while the calcified zone secures cartilage to bone. These four zones give rise to a functionally graded material, with collagen fibrils gradually changing their orientation, which is ideally designed to have a shear resistant surface providing smooth contact on one side and be solidly attached to bone on the other.

Articular cartilage forms a thin layer (0.5–5 mm) on the ends of long bones in a synovial joint. In addition to providing a smooth, nearly frictionless surface for joints to slide on, it distributes the loads and transfers it across bones. Dynamic loads amplify the impact forces acting on the joints. The fluid has a significant impact on the properties of cartilage. The pressurization of water gives the articular cartilage the ability to withstand dynamic loads, often as high as several times one's body weight. The presence of a fluid, which can be considered as incompressible, plays an integral role in resisting and damping the loads. Thus, cartilage is a porous solid filled with fluid. Macroscopic properties of cartilage depend on the movement of fluid flowing in and out of pores during the deformation, resulting in a complex non-linear and time-dependent behavior [52]. Articular cartilage is a non-linear viscoelastic/viscoplastic, or more accurately poro-viscoelastic material. In poroelasticity theory, mechanical loading gives rise to pressure gradients in fluid-filled pores [45].

3.4. *Mineralized systems*

The biological systems discussed so far are composed almost exclusively of protein or fibrous constituents. Mineralized systems incorporate a stiff ceramic phase in conjunction with these tough biopolymers, allowing for the creation of complex composite arrangements with impressive properties. Many mineralized systems such as the shells of marine organisms, turtle carapace, and bone (especially the skull) are defensive armors that are used to protect internal tissue. Other mineralized systems are utilized for more specified offensive functions, like the hammering of wood by the woodpecker beak or smashing of shells by the mantis shrimp dactyl club. Both offensive and defensive systems have evolved an intriguing range of structures to improve impact resistance.

3.4.1. *Bony systems*

Bone is a connective tissue that, among its other functions, serves as structural support for soft tissues in the body and protection of organs. As a structural material, bone has excellent properties: high stiffness, strength, toughness, energy absorption, while also being lightweight. These impressive properties are due to bone's composite, spatially heterogeneous, and hierarchical structure [45,53].

At the macroscale, bone consists of cortical (compact), low-porosity bone forming an outer shell and cancellous (trabecular), highly porous bone filling space between or at long bone's ends. Such structure is optimal as it allows the body to withstand high functional loads while minimizing weight. The porous network at the ends of the bone distributes loads at joints. Bone is a composite material that at the nanoscale is made of soft and deformable organics (mainly collagen) and stiff but brittle apatite minerals, with about 1:1 ratio by volume, and fluid-filled pores. Collagen fibrils are mineralized with nanoscale crystals forming mineralized collagen fibrils, which align preferentially into a single lamella. These lamellae arrange in layers at the microscale to form trabeculae in cancellous bone and osteons embedded in interstitial bone in cortical bone. Osteons are hollow cylinders made of concentric helically-wound lamellae. At mesoscale, a network of struts forms trabecular bone while osteons embedded in interstitial bone form cortical bone [53]. Osteons align in long bone's axis to carry loads and absorb impacts due to running and other dynamic activities. Lamellar structures deflect cracks at interfaces.

Stress–strain curves of cortical bone show a linear portion followed by a non-linear region once the yield stress is reached. Human cortical bone (with 5–30% porosity by volume) is transversely isotropic and has a longitudinal elastic modulus of 5–20 GPa in the long bone direction. Trabecular bone (with up to 90% porosity) exhibits a typical porous material response with an initial linear portion, followed by a plateau due to compaction of trabeculae, before an increase after compaction [54,55]. Bone has been mostly studied as a linear elastic and elasto-plastic material [56,57]. However, it has time-dependent properties, so it is viscoelastic and viscoplastic [54,58]. Bone is fluid filled so it can also be considered as a poroelastic material.

The turtle shell is composed of fused bone covered in keratin scutes [59]. These keratin scutes easily delaminate and deflect cracks, toughening the shell before the load reaches the more brittle bone [60]. As the most likely region to experience high impacts from predators, the upper section of the shell, called the carapace, has been the focus of most structure–property research. The box turtle carapace is composed of two firm, exterior, cortex layers, with a porosity of ~7%, sandwiching an interior, closed-cell, cancellous layer with a porosity of ~65%. The Young's modulus of these layers is approximately 20 GPa and 1 GPa, respectively. Compression tests reveal familiar sandwich structure behavior (Fig. 4A); a small linear elastic regime as the closed cells in the foam layer resist buckling, followed by a plateau where the pores collapse, after which another linear elastic regime is evident as the foam densifies and damage occurs. Samples that contained all three layers of the turtle carapace performed better than samples that were composed of just a single exterior

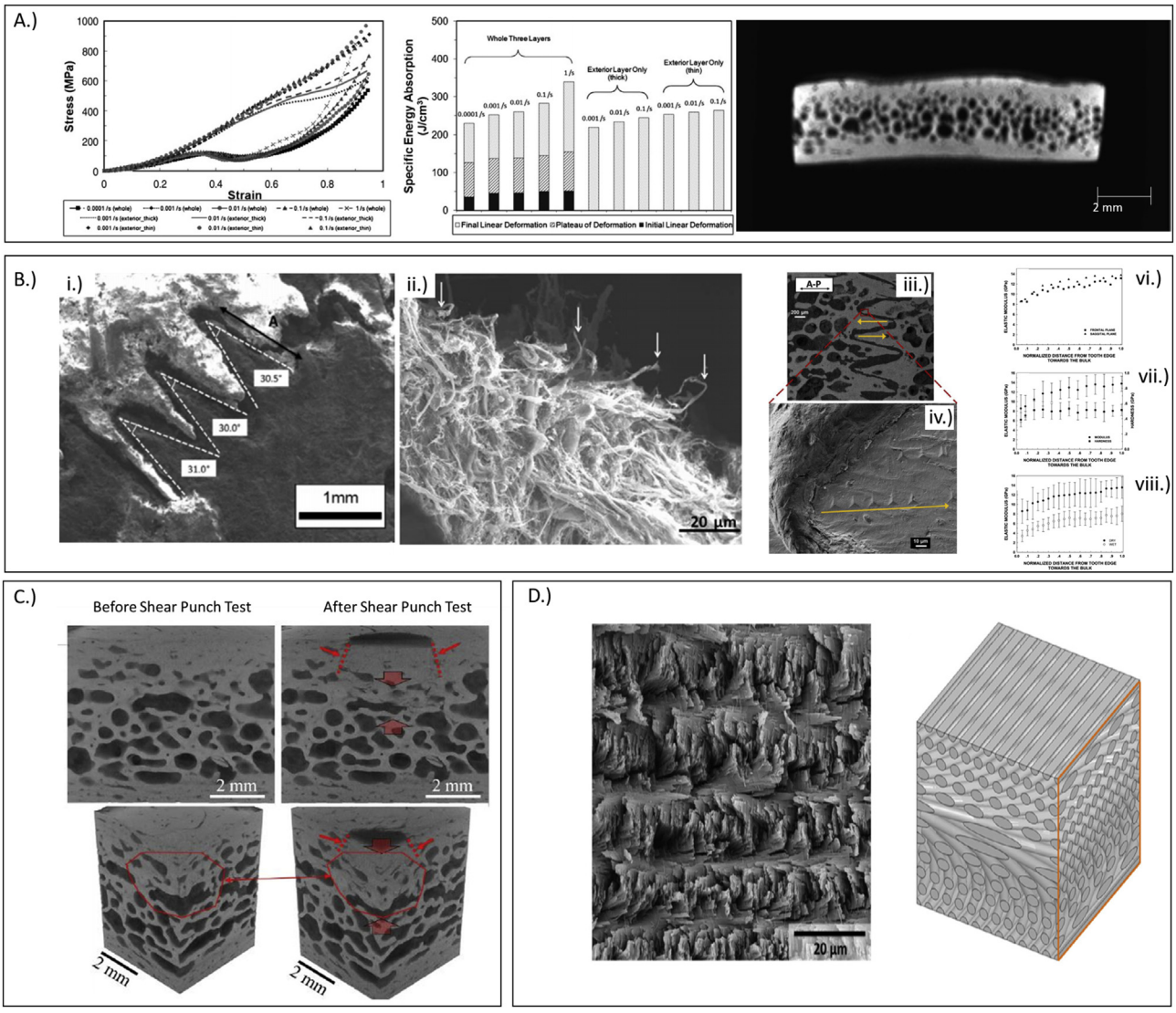

Fig. 4 – A) (Left) Stress–strain curve of turtle shell samples at various strain rates and locations. The upper curve represents samples taken from just the exterior portion of the shell that has minimal porosity. The lower curve represents samples that include all three layers of the turtle shell's sandwich structure. (Middle) The three-layer samples have a higher energy absorption by volume than the single layer samples. This bar chart also shows how much energy was absorbed in each deformation regime. (Right) A cross section of the turtle shell where the three layers can be easily observed [61]. B) Interlocking sutures. (i) The interlocking sutures found between osteoderms in the turtle carapace allow the shell to flex without fracturing, but also provide an energy absorbing mechanism during failure. (ii) When the sutures are pulled apart the collagen network holding it together is stretched before the fibers fracture. Fractured fibers are marked by the white arrows [62]. (iii-viii) Sutures in the red-eared slider turtle have a gradient in elastic modulus. (iii,iv) Nanoindentation tests were performed moving from the tip of the suture tooth to the bulk of the turtle shell. (vi-viii) The elastic modulus decreases towards the tip of the suture teeth in wet and dry conditions [60]. C) Skull section prior to and after punch test. Conical damage zone after impact indicates that the porous structure recruits nearby material to resist the load. Post-test image also shows densification mechanism that is common in sandwich structures [65]. D.) SEM image of Bouligand structure in Mantis shrimp dactyl claw (left) and 3D representation of the Bouligand structure (right) [123]. Adapted with permission [61] Copyright 2009, Elsevier. Adapted with permission [62] Copyright 2015, Acta Materialia. Adapted with permissions [60] Copyright 2012, Acta Materialia. Adapted with permission [65]. Adapted with permission [123] Copyright 2014, Acta Materialia.

layer under compression; the latter exhibited near-linear stress–strain curves. The three-layered samples, pictured on the right side of Fig. 4A, absorbed more energy compared to single-layer exterior plate samples and both absorbed more energy as strain rate increased. The specific energy absorbed for each type of sample at different strain rates can be seen in the center of Fig. 4A. Comparison with the entire turtle carapace showed that it responds to flexure in a very similar way to the smaller specimens, with the same stress–strain and energy absorption trend [61].

The turtle carapace also has a porosity gradient through the cancellous layer, which is hypothesized to prevent stress concentrations at the interface of the porous and non-porous layers. The bones, called ribs, are fused together to form the turtle's shell and are connected by a soft, unmineralized collagen layer; the interface forms a suture structure and is highly flexible as seen in Fig. 4B (i). Under small loads, these interfaces allow the shell to flex and deform but lock together and stiffen under higher loads. These sutures are thought to trap and arrest laterally propagating cracks. When pulled apart the collagen network connecting the interlocking sutures, stretches and ruptures absorbing energy in the process. Fig. 4B (ii) shows the ruptured collagen network after tensile tests. White arrows indicate torn collagen fibers [62]. To prevent fracture of the suture teeth during impact, another gradient, this time in stiffness, was measured between the flexible suture material and the rigid bone in the center of the carapace. Fig. 4B (iii, iv) shows the path of nanoindentation tests that produced the plots shown in Fig. 4B (vi-viii). These tests revealed a steady increase in elastic modulus from the tip of the teeth towards the bulk of the turtle shell, even under wet conditions [60]. This gradient is also thought to induce more intimate entanglement of the sutured interface, improving interlocking under high loads. Finally, the cortex layers have different fibrous structures. The upper cortex layer is close to the point of impact on the shell and thus is thought to be optimized to toughen the shell and prevent cracking while the lower cortex layer is believed to mainly provide structural support. The upper layer is composed of a randomly oriented osteon network embedded in an interwoven fibrillar array. This disordered arrangement hinders crack initiation and confines larger cracks from spreading through the material. The lower cortex layer has orthogonally aligned fibers which provide biaxial support at the base of the shell, but are less impact resistant [60].

The full ramifications of a bony sandwich structure under impact have been further explored in testing on the human skull, which has a thicker, trabecular layer with irregular pores sandwiched between high-density cortical bone [63,64]. Under impact, Wu et al. [64] observed that, at low velocities ~3–4 m/s, round impactors simply rebounded off of the skull, failing to puncture the firm external cortical bone. As impact speed increased though, the skull absorbs more energy, just as the turtle carapace does – this is in part due to the ability of the skull structure to widen the impact region. At high velocities, the damage area of the skull bone grows, indicating that more material becomes involved in absorbing energy and resisting the impact [64]. Brown et al. [65] performed shear punch tests at strain rates of $0.001s^{-1}$ and $0.1\ s^{-1}$ on the human skull to better understand its dynamic shear strength and deformation. They found that shear strength of the individual layers of the skull had minimal dependence on strain rate, but when tested together, the skull had a higher shear strength at higher strain rates. In general, the porous trabecular bone determined the shear strength of the specimens. At both strain rates they observed pore collapse and densification in the central region of the skull bones. A conical damage and densification zone was also observed beneath the impact surface (Fig. 4C), indicating that the porous structure of the skull spreads the impact over a larger and larger area as the energy moves through the skull thickness. This recruits more material to resist the stressed state and prevent damage [65].

Additionally, the skull has a gradient in its porous arrangement [63]: Brown et al. [65] reported a pore volume fraction of the inner and outer layers of the skull to be ~10% which gradually increases to nearly 50% in the center of the skull bones [65]. Similar to porous gradients in fruits and nuts discussed earlier, this gradient decreases stress concentrations and the likelihood of delamination between layers of differing properties.

The woodpecker skull has been widely investigated with respect to impact [4]. Dissimilar to mammalian skulls, the sandwich structure is filled with air to reduce its weight for flight. Spongy porous bone coalesces at the countercoup position of the beak and is expected to evenly distribute impact stress, preventing damage to the brain [66]. There exists a gradient in Young's modulus across the skull from 4.0–11.0 GPa which has been modeled to minimize the peak stress during impact [67–69]. There is an additional impedance mismatch in the hyoid apparatus (the bone which suspends the tongue and wraps around the back of the skull) in the transverse and longitudinal directions. This gradient, along with the geometric tapered effect, and the surrounding viscoelastic tissues have been shown to mitigate the stress wave propagation through viscoelastic dampening [70,71].

The woodpecker beak can be imagined as a sandwich structure with three layers: (1) the rhamphotheca composed of compliant keratin surrounding, (2) spongy trabecular bone with (3) compact bone in the center. At the micro-scale, the keratin cells in the rhamphotheca stack up in layers along the impact direction and neighboring cells have an interlocking suture interface that are on the order of nanometers. The waviness (the height-to-width ratio) of the suture is ~1. The hardness and elastic modulus mismatch between the three layers in the beak help to dissipate internal stress. Additionally, the viscoelastic muscles in the neck and legs dampen the impact energy.

The elk antler has a similar structure to that of bone, with vascular channels (~15–25 μm diameter) surrounded by concentric bone lamellae, collectively referred to as osteons. Using drop tower experiments, Lee et al. [38] determined that elk antler had higher impact strength than nacre. Launey et al. [72] claimed that the main energy dissipation mechanisms in the elk antler arise from microcracks that form at these

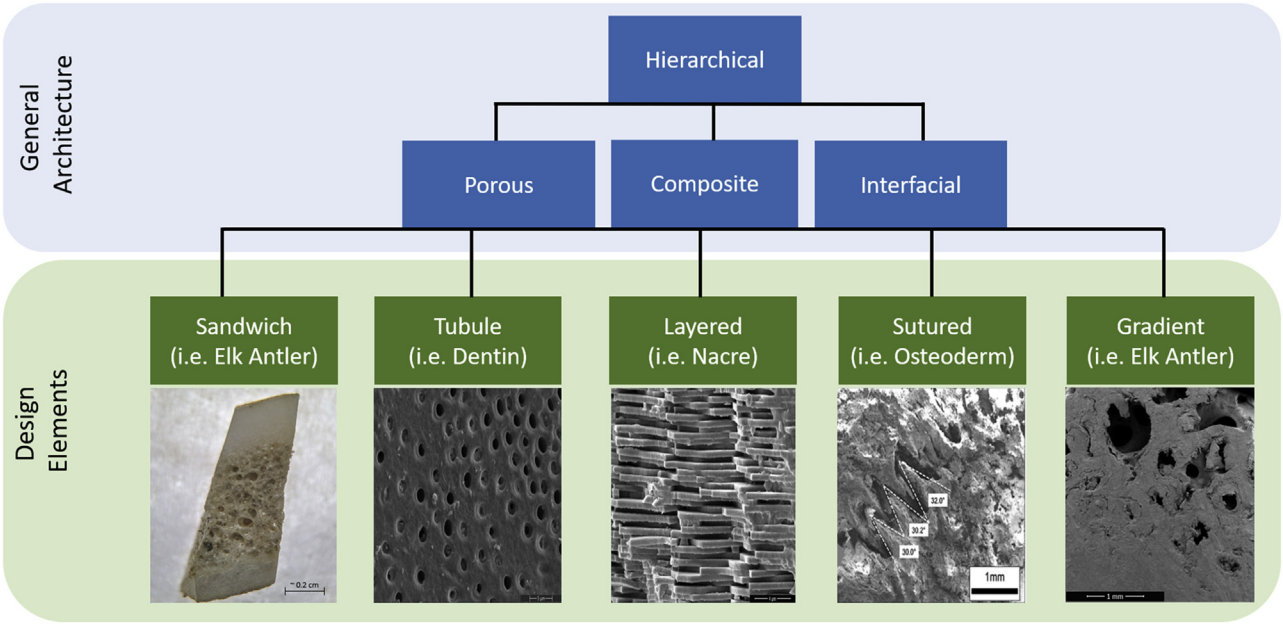

Fig. 5 – General architecture and specific design elements found in biological materials and, more particularly, impact resistant materials. (Top) Four general features found in all biological materials that are especially important for impact resistance. All biological materials are hierarchical. These hierarchies are composed of various arrangements of composite materials, pores, and interfaces. (Bottom) Five micro- and meso-structures that are commonly found in impact resistant biological materials and have been shown to improve performance under dynamic loading. These include sandwich, tubule, layered, sutured [62], and gradient structures. Adapted with permission [62] Copyright 2015, Acta Materialia.

lamellar boundaries. These microcracks lead to crack deflection and bridging, in a similar fashion to nacre. Unlike nacre, the cracks in the elk antler twist when they reach these interfaces, which absorbs more energy [72].

3.4.2. *Marine organisms*

The conch shell has a similar composition to that of the nacre found in abalone; however, it has a hierarchical cross-lamellar structure that makes it an order of magnitude tougher. Both materials are made of mineralized calcium carbonate sheets glued together by a protein phase, but the conch shell has three different hierarchies of lamellar layers which crisscross the layers above and below [73]. This leads to a compartmentalization of cracks which are arrested at the rotated interface between layers. In quasi-static testing, the conch shell also dissipates energy by forcing cracks to meander (similar to the phenomenon found in nacre [181,182]) and by allowing microcracking to occur in the

Table 1 – Comparison of characteristics present in impact resistant biological systems.

Biological System	Sandwich	Tubular	Layered	Suture	Gradient	Hierarchical	Composite	Interfacial	Porous	Viscoelastic/ Viscoplastic
Pomelo	+	–	+	–	+	+	+	+	+	+
Coconut	+	–	+	–	+	+	+	+	+	+
Wood	+	+	+	–	+	+	+	+	+	+
Hooves	+	+	+	+	+	+	+	+	+	+
Horns	+	+	+	–	+	+	+	+	+	+
Pangolin Scales	–	–	+	+	–	+	+	+	+	+
Tendon	–	–	+	–	–	+	+	+	+	+
Ligament	–	–	+	–	–	+	+	+	+	+
Cartilage	–	–	+	–	+	+	+	+	+	+
Bone	+	+	+	–	+	+	+	+	+	+
Turtle Carapace	+	–	+	+	+	+	+	+	+	+
Human Skull	+	–	–	+	+	+	+	+	+	+
Woodpecker Skull	+	–	–		+	+	+	+	+	+
Woodpecker Beak	+	–	+	+	+	+	+	+	+	+
Elk Antler	–	+	–	–	+	+	+	+	+	+
Conch	–	–	+	–	–	+	+	+	+	+
Mantis Shrimp	–	–	+	+	+	+	+	+	+	+

weaker phase which delocalizes damage [74]. However, unlike nacre which performs poorly during impact [38], the conch shell has several high strain-rate strengthening mechanisms that are not observed during quasi-static tests. At a strain rate of 10^3 s^{-1}, the conch shell has a 67% higher fracture strength than when tested at a strain rate of 10^{-4} s^{-1}. Under impact loading, the third order lamellae (the smallest of the hierarchical lamellae) fracture and splinter away from the rest of shell. In this case, fracture no longer occurs along lamellar interfaces but instead cracks through the lamellae creating a powder of fragmented nanorods. Within a given third order lamella, impact strain rates were shown to induce rotation in nanoparticles which can block dislocation activities and improve fracture strength. Further, trapped edge dislocations were observed after impact suggesting more strain rate dependent dissipation mechanisms that are not seen during quasi-static tests [75].

One of the most remarkable impact resistant biological structures is the dactyl club of the mantis shrimp, which strikes its prey at a velocity of up to 23 m/s. Beneath the dactyl club's highly mineralized surface are oriented chitin fibers that form a twisted Bouligand structure. The Bouligand structure is composed of superimposed layers of fibers whose orientation is rotated relative to the layers above and below, thereby creating a helical, stacked plywood arrangement. These are visualized in Fig. 4D. Early pioneering work by Bouligand and Giraud-Guille [76] described this twisted, layered arrangement in a wide variety of organisms ranging from crustaceans to insects to bacteria, but more recent work has probed the mechanical functions of these structures. When this underlying phase in the mantis shrimp begins to fracture, cracks travel in a helicoidal path between the layers of fibers. Another implication of this structure is that crack fronts twist as they propagate creating larger fracture surfaces which absorb more energy than flat cracks [77].

4. Recurrent impact resistant structures and material properties in nature

Through the examination of successful biological systems which undergo impact, it becomes evident that there exists several reoccurring design elements and material properties that are responsible for successful impact resistant systems. The specific structural elements are categorized as: *sandwich, tubular, layered, sutured, and gradient*, all of which are employed in global features (hierarchical, composite, porous, and interfacial). These key design elements are displayed in Fig. 5. In all of these structural arrangements, the viscoelastic and viscoplastic material properties have an important influence on the energy absorbance and dissipation capabilities.

4.1. *Structural elements found in impact resistant biological systems*

The designs discussed here do not occur in isolation, but rather in concert across various length scales within a single biological system. Table 1 identifies the frequency of each these structures with respect to the biological systems reviewed in Section 3. As mentioned earlier, all biological materials are viscoelastic/viscoplastic, hierarchical, composite, porous, and have defining interfaces due to their growth from the molecular level to the macroscale and their reliance on basic polymeric and mineral subunits. Gradient structures

Table 2 – Summary of impact resistant design elements and material properties.

Impact Design Element/Material Property	Energy Absorbing Mechanisms	Tailorable Designs	References
Hierarchical	Each layer works synergistically for an enhanced overall effect. Any of the energy absorbing mechanism detailed below can be found across multiple levels.	Increasing hierarchical ordering, incorporation of multiple structural elements, length scale	[99–101]
Sandwich	Fracture and wrinkling in the top face; core buckling, densification, and shearing; viscoelastic dampening, strain energy storage	Face thickness to core thickness ratio, geometric cell structure of core, addition of fluid to the core, gradient in density and cell size	[102–111]
Tubular	Buckling, collapse, delamination, crack deflection	Size, shape (circular vs elliptical), volume fraction, addition of reinforcing layer, gradients in density and diameter, loading direction	[112,113]
Layered	Microbuckling, delamination, crack deflection, shearing between layers, microcracking	Lamellar arrangement (layered, hexagonal concentric, rotated ply etc.), geometry of the interface (wavy)	[114,115,117,118,120–124,126]
Gradient	Fracture energy, crack deflection, localized pore collapse	Continuous gradient, step-wise gradient, porosity gradient	[127–136]
Suture	Attenuate impact stress, reduction of pressure waves through the conversion of compression to shear	Geometry of suture (sin wave, triangular, trapezoidal), degree of waviness (Amplitude, wavelength, frequency), loading direction, additional hierarchies	[142–144]
Viscoelastic and Viscoplastic	Viscoelastic and viscoplastic deformation, vibrational dampening	Ratio between elastic and viscous response, degree of hydration, temperature	[23,83–87]

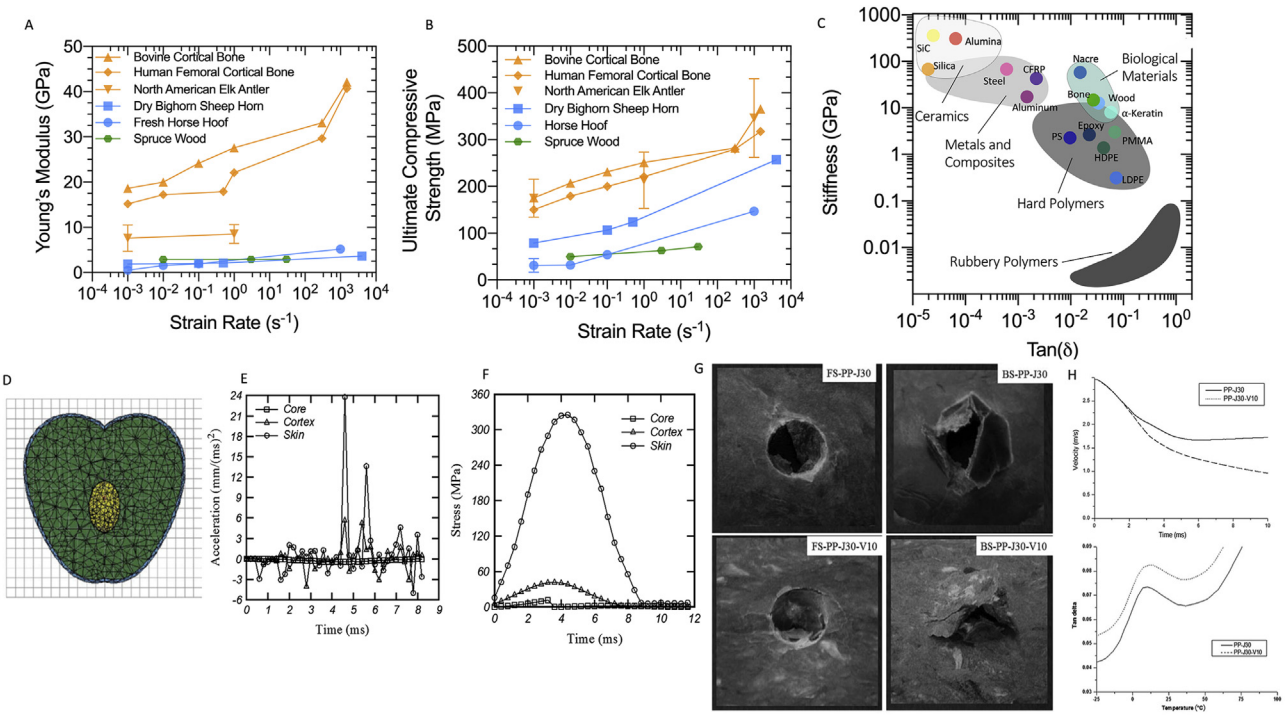

Fig. 6 – Inelastic behavior of biological materials. A) Strain rate dependence with respect to Young's Modulus for representative biological systems. Hydroxyapatite/collagenous systems of bovine and human cortical bone and elk antler (yellow), keratinous systems of bighorn sheep horn and horse hoof (blue), and cellulose/hemi-cellulose/lignin system of spruce wood (green) B) Strain rate dependence with respect to ultimate compressive strength. C) Ashby plot of stiffness and damping (tan(δ)) which indicates the enhanced performance of biological materials compared to engineering materials. D-F) FEA of apple layers under impact loading (1 m/s). D) Organization of the three layers: skin (light blue), cortex (green), and core (yellow). E) Acceleration with respect to time of the three layers. F) Stress with respect to time of the three layers [86]. G-H) Addition of viscose fibers to PP-jute affects impact response and viscoelasticity. G) (Top) Front side (FS) and back side (BS) of PP-jute after low-velocity falling-weight impact test. (Bottom) Front side (FS) and back side (BS) of PP-just added viscose after low-velocity. H) (Top) Impact velocity with respect to time. Indicating how the addition of viscose fibers decreases residual velocity. (Bottom) Tan delta with respect to temperature. Indicating how the addition of viscose fibers increases the damping ability [87]. Adapted with permission [86] Copyright 2016, Elsevier. Adapted with permission [87] Copyright 2015, Wiley.

also exist in nearly all of the biological systems reviewed in this paper, often occurring at transitions between interfaces. Layered arrangements are incredibly common and have been shown to provide a wealth of energy absorption mechanisms; again this is often a result of natural layer-by-layer growth mechanisms. Other structures such as suture interfaces, sandwich, and tubular arrangements appear to be more situational. These structures often involve compromising other properties such as stiffness or isotropy. The dragonfish tooth is a perfect illustration of this compromise. Tubules are commonly found in the dentin layer of teeth and are known to strengthen the material under loading by deflecting cracks. However, the dragonfish has developed teeth that do not have dentin tubules. Velasco-Hogan et al. [55] suggest that this is meant to decrease the amount of light scattered by the teeth, allowing the dragonfish to evolve ones that are uniquely transparent an important adaptation for camouflage and hunting in the deep sea. Similarly, all biological materials are multifunctional and must meet a variety of demands for evolutionary success which might not lead to the optimization of specific functions such as impact resistance.

Furthermore, each of these designs have different failure and energy absorption mechanisms as well as different parameters than can be tailored. Sandwich and tubular arrangements absorb significant amounts of energy through elastic deformation, collapsing and then rebounding to their original shape at impressively large strains. However, tubules and pores can also act as flaws leading to high stress concentrations at their edges and causing premature fracture. On the other hand, layered and suture structures are fantastic at deflecting cracks and absorbing energy through plastic deformation such as suture delamination or lamellar slipping. Section 5 examines each of these structural design elements individually, focusing on important parameters that determine their impact resistance and bioinspired studies that have probed the nature of each design element. These finding are summarized in Table 2.

4.2. *Time-dependent behavior*

Due to their biopolymeric constituents (collagen, keratin, cellulose, hemi-cellulose, lignin, and chitin) biological

materials demonstrate time-dependent behavior with respect to elastic modulus, strength, and post-yield behavior. Depending on the polymer, increasing strain rate can influence changes in mechanical behavior. For keratin, with increasing strain rate the mechanical behavior transitions from elastic to ductile-plastic to brittle fracture [15]. This is attributed to the time scales that are required to rearrange, slide, and stretch fibers through the breaking of intermolecular forces and chemical bonds [42,78]. Generally, biopolymers become stiffer and stronger and show decreasing breaking strain as strain rate increases (Fig. 6 (A,B)). The strain-rate sensitivity of the elastic modulus and ultimate compressive strength in biopolymers can be seen in Fig. 6 (A,B) which demonstrates this phenomen for collagen/hydroxyapatite (cortical bone and elk antler) [79,80], keratin (bighorn sheep horn and horse hoof) [32,41], and cellulose/hemi-cellulose/lignin (spruce wood) [81] systems. This rate-dependent behavior has important implications for impact resistant biological materials suggesting that under dynamic conditions these materials can withstand greater stresses and have different failure mechanisms when compared to quasi-static conditions. Additionally, temperature, hydration, and loading orientation are shown to influence the degree of strain rate sensitivity. Temperature can change the activation barrier for structural transformations (e.g., sliding and rotating) of polymeric units to occur. Hydration or the increase in water content leads to a change in viscosity of the material and its ability to dampen the travelling stress waves [41]. For the bighorn sheep horn, it was shown that at lower strain rates (10^{-3} – 10^{-1} s^{-1}) there is a significant difference in the compressive stiffness with respect to loading direction (longitudinal and transverse were greater than the radial direction), while there was no significant difference between all three directions at higher strain rates (4×10^{3} s^{-1}) [41].

Inherent material properties are important determiners in providing energy absorption mechanisms that allow for impact resistance with a primary dependence on viscoelasticity and viscoplasticity. Viscoelastic materials are characterized as having both an elastic and viscous response. A purely elastic material stores mechanical energy during deformation and upon unloading the stored energy is released, allowing the material to return to its original shape. Viscosity describes a materials resistance to flow and upon loading, energy is dissipated as heat. Viscoelastic stress–strain behavior is time-dependent. Viscoelastic materials work to isolate impact by attenuating shock and damping vibration. During impact, energy can be stored and dissipated as viscoelastic deformation. Viscoelasticity is described by the loss modulus (stored elasticity), storage modulus (energy dissipated as heat), and tan (δ) (the ratio between storage modulus and loss modulus which represents damping). For structural materials, it is advantageous to have high stiffness

Table 3 – Summary of dynamic testing techniques and strain rates on biological systems.

Biological System	Drop tower	Hopkinson bar	Compression test	Tensile test	Flexural test	Shear Punch test	Other
Pomelo	–	–	5 mm/min [21]	–	–	–	(free fall) 10.85 m/s [21]
Coconut	–	–	–	0.3 mm/min and 0.6 mm/min [22]	–	–	–
Wood	1.6 m/s [23]	–	12 mm/min [23]	–	–	–	–
Hooves	–	1000 s^{-1} [32]	2.5–1.7 × 10^{-5} m/s [30], 0.1s^{-1},0.01s^{-1}, 0.001s^{-1} [32]	5 mm/min [36], 8.3 × 10^{-5} m/s [34], 2 mm/min [28]	–	–	–
Horns	>3.8 m/s [38], 4.4 m/s [39]	4000 s^{-1} [41]	0.5s^{-1}, 0.1s^{-1}, $10^{-3}s^{-1}$ [41], 3 mm/min [39]	2 mm/min [31]	2 mm/min [31]	–	–
Pangolin Scales	–	–	10^{-3} s^{-1} [26]	10^{-1} – 10^{-5} s^{-1} [26]	–	–	–
Tendon	–	–	–	5, 0.5, 0.05% s^{-1} [173]	–	–	–
Ligament	1.5 m/s [174]	–	–	–	–	–	(Impactor Trolley) ~1 m/s [175]
Cartilage	1500-740 s^{-1} [176], 1, 0.75 m/s [177]	–	–	–	–	–	–
Bone	–	6.1 m/s [178]	1500 s^{-1} – 0.001 s^{-1} [79], 0.6 mm/min [178]	–	–	–	–
Turtle Carapace	–	–	10^{0}–10^{-4} s^{-1} [61], 10^{-3} s^{-1} [62], 2 mm/min [179]	–	0.5 mm/min [60]	–	–
Human Skull	8–7.1 m/s [180]	–	2.5 mm/s [180]	–	–	0.1 and 0.001 s^{-1} [65]	–
Elk Antler	>3.8 m/s [38]	–	–	–	0.9 mm/min [72]	–	–
Conch Shell	–	1383 -1686 s^{-1} [75]	10^{-2} – 10^{-4} s^{-1} [75]	–	0.1 mm/min [74]	–	–

for rigidity with high mechanical damping (tan (δ)) [82]. Fig. 6C shows the relationship between stiffness and damping of conventional materials and highlights the excellent performance of biological materials. Viscoplastic materials are time-dependent and deform permanently. Such permanent changes may be due to sliding of interfaces, microcracking, and delamination, leading to energy dissipation.

Many impact resistant biological materials utilize viscoelasticity as a way to effectively store and dissipate energy under dynamic conditions. The viscoelastic response of the muscle and tissues surrounding the hyoid apparatus found in the skull of the woodpecker is known to reduce stress waves during free vibration induced by pecking [83]. Articular cartilage, when subjected to high-speed loading, behaves as a viscoelastic material which provides a mechanism for energy dissipation that limits potential damage to the matrix or surrounding tissues [84]. While all biological materials have some degree of viscoelasticity, there are competing energy absorption mechanisms at high strain rates that often dominate over viscoelastic deformation. For example, while wood has a strong viscoelastic response under quasi-static conditions, the structuring of layers and voids ultimately determines its energy absorption mechanisms under impact [23].

Fruits such as pomelos [85] and apples [86] absorb dynamic waves when dropping from trees and the capacity to dissipate energy is shown to depend on the viscoelastic properties of the protective layers. Ahmadi et al. [86] performed finite element analysis to study the dynamic behavior of an apple and its corresponding layers (skin, cortex, and core) under impact loading (Fig. 6 (D-F)). The skin was modeled as an elastic material (E: 12 MPa, ν: 0.35), while the cortex (E: 5 MPa, ν: 0.35, G_0 :0.15, β: 1/800) and core (E: 7 MPa, ν: 0.35, G_0 :0.15, β: 1/800) were represented as viscoelastic materials. The apple collided with a rigid plate at a velocity of 1 m/s. As shown in Fig. 6 E and F, the skin has the largest stress and acceleration under impact, while the cortex and core stresses are minimized due to their viscoelastic response. Here, viscoelastic deformation and energy dissipation are important in reducing localized damage.

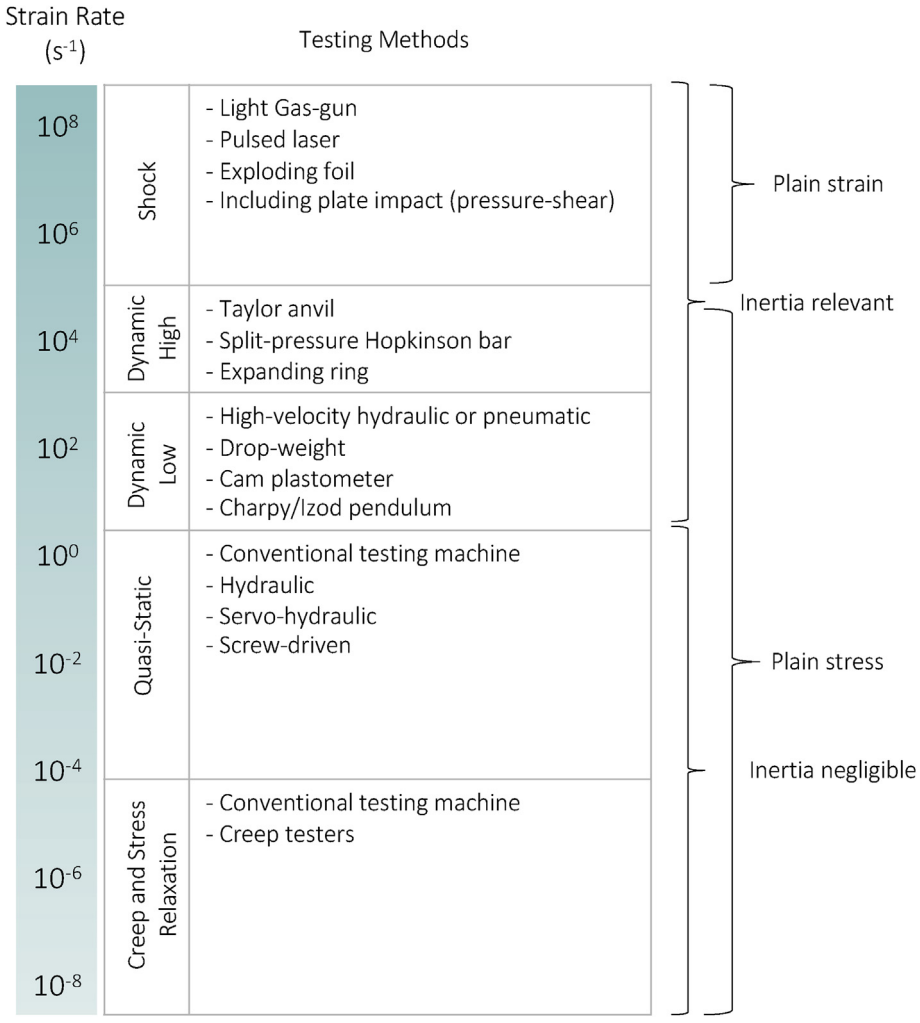

Fig. 7 – Testing methods and their achievable strain rates.

4.2.1. *Relationship between impact toughness and damping behavior*

Ranganathan et al. [87] investigated the relationship between impact toughness and viscoelasticity of polypropylene (PP)-jute composites with the use of viscose fiber (rayon fiber from regenerated cellulose). Charpy impact testing and low-velocity drop-weight impact tests were used to determine impact resistance and dynamic mechanical analysis was used to quantify viscoelasticity. The addition of viscose (PP-J30-V10) increased the Charpy impact strength from 3.2 kJ/m^2 to 7.5 kJ/m^2 and decreased the residual impact velocity from 1.7 m/s to 0.9 m/s (Fig. 6 (G,H)). Images of the front and back sides of the low-velocity falling-weight impact tests show less damage for the composite with added viscose. Dynamic mechanical analysis showed that the addition of the viscose fibers decreases the storage and loss modulus, softening the material, making it more deformable and increasing the loss tangent (tan (δ) = loss modulus/storage modulus), which describes the dampening behavior. The addition of the viscose fibers improved impact performance by effectively dampening energy. While there is much more to take into consideration, such as microstructure and interfacial properties, this study sheds light on how viscoelastic properties can influence impact toughness by improving the materials dampening ability.

4.3. *Testing methodology*

To understand the impact resistance of biological materials researchers have utilized a number of different mechanical tests. These tests differ in their ability to consider different loading conditions, loading orientations, and strain rates. With materials that are highly anisotropic (i.e. dry big horn sheep horn [41]) or strain rate sensitive (i.e., bone [79]), it is important to test materials in a number of different orientations over a broad range of strain rates. Table 3 compiles different testing methods and strain rates used to examine the impact resistance of biological materials in the preceding sections. This table does not provide an exhaustive list of all testing done on these systems but provides an idea of what work has been done.

One of the most popular testing techniques is the drop tower, which is capable of reproducing impacts that occur in the natural regime (<25 m/s). These experiments are useful for understanding the energy absorption and damage tolerance of a material and are good for comparing different materials tested under the same conditions. However, drop towers have a number of important variables that can make it difficult to compare results between different studies. These include sample size, clamping mechanism, and indenter shape and size. For very high strain rate tests and insight into stress–wave interaction in a sample, Hopkinson bar tests have been utilized to examine biological materials. These tests give unique insight into a material's response to dynamic loading but can be expensive [41] and may necessitate modifications for low impedance materials, which is characteristic of biological materials. These modifications involve using bars with the proper impedance mismatch ratio relative to the sample such as woven glass epoxy composite, PMMA, or magnesium alloy bars [41,88]. Further, a pulse shaper is often used to ensure stress equilibrium and homogenous deformation in the sample [41,89]. The most popular testing methods for impact resistant materials are simple compression, tensile, and flexural tests, often using a universal testing machine. As has been examined in previous sections, these tests are restricted to strain rates below the dynamic, impact regime (~1-2 s^{-1}) but can provide insight into deformation and fracture mechanics. The allure of compression, tensile, and flexural tests is their ease of use and simplicity. These tests can provide valuable material parameters such as elastic modulus, Poisson's ratio, fracture toughness, or ultimate strength (even though these may vary with strain rate). Different strain rates can still be accessed using these simple techniques and important strain rate dependent trends can be observed. Free-fall experiments (where the sample is dropped onto a surface rather than a weight onto the sample as in drop tower experiments) and shear-punch tests are used much more sparingly than other testing methods and were only examined in this review for the pomelo and human skull, respectively. There are other techniques for quantifying impact resistance, such as Izod and Charpy testing, but these have not been as widely used to study biological materials mostly in part due to samples being too small.

For lower strain rate tests (<10^0 s^{-1}) the inertia of the sample can be ignored, but for higher strain rates experiments must take into account the force required to accelerate a material to high deformation speeds. Above 10^0 s^{-1}, the force is not simply dictated by the material's intrinsic strength. Inertial effects are also greater in larger samples [90]. Another consideration for high and low strain rate testing is the use of plane stress approximations. In shock tests that involve strain rates $\geq 10^6$ s^{-1} this approximation breaks down and plane strain must be used. Fig. 7 shows the achievable strain rates for a variety of mechanical tests, including each of the tests discussed in this section. The figure also indicates the strain rate thresholds for plane stress approximations and disregarding inertial effects of the sample.

5. Exploration of structural elements for impact resistance

It is evident that natural materials profit from the combination of structural design elements and many levels of hierarchy which are constructed via self-assembly [17]. However, this makes it difficult for testing to probe the role of individual structural designs (i.e., sutures, tubules, etc.) within a biological material. Many researchers have turned to computational modelling [91–94] and additive manufacturing [95–98] to recreate and test simple materials with only a single structural feature, before moving on to more complex models [96]. This allows them to better understand the role of each design element and the synergistic effects that arise when they are combined.

5.1. *Hierarchical*

All biological materials are inherently hierarchical due to their bottom up development; simple molecules combine into

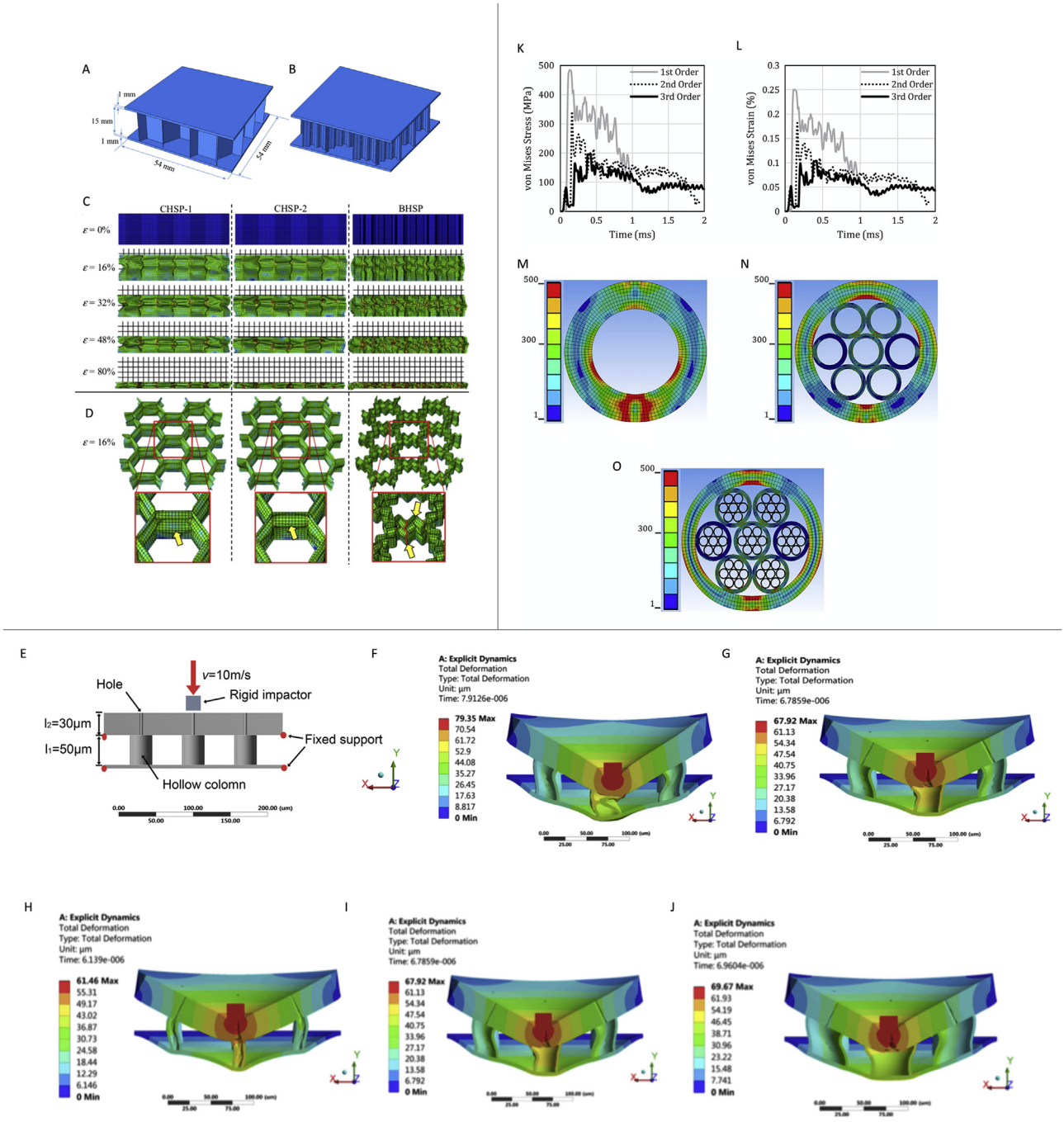

Fig. 8 – Impact modeling of bioinspired sandwich and tubule structures. A-D) Impact modeling of a wavy bioinspired honeycomb cell compared to a conventional honeycomb cell. A) Schematic of the conventional honeycomb cell with flat walls (CHSP-1). B) Schematic of the bioinspired cell with wavy walls (BHSP). C) The three investigated designs (CHSP-1, CHSP-2, and BHSP) and deformation at various strains. D) The deformation of the cell walls of the three designs zoomed in at a strain of 16% [107]. E-J) Impact testing of bioinspired tubule structures. E) Schematic of the cuticle layer with tubules (holes) supported by larger tubules (hollow columns). F) Deformation of the cuticle layer without tubules (holes). G) Deformation of the cuticle layer with tubules (holes). H-J) Deformation of the tubule structure with increasing inner diameter [112]. K–O) Impact results of the tubular structure with increasing hierarchical order. K) Impact response and von Mises stress of the three orders of hierarchy. L) Impact response and von Mises strain of the three orders of hierarchy. M) Deformation map of the first order single tubule. N) Deformation map of the second order which is a tubule with seven tubules within. O) Deformation map of the third-order structure [113]. Adapted with permission [107] Copyright 2019, Springer. Adapted with permission [112]. Copyright 2018, Springer. Adapted with permission [113]. Copyright 2018, Elsevier.

larger constituents until a functional macroscale component is formed. These levels of hierarchy improve the properties of biological structures in ways that traditional materials cannot. Xu [99] reviews the many processes that have been developed for manufacturing hierarchical materials and categorizes them into three primary groups: porous materials, structural materials, and smart materials. Of these, research in porous materials have seen the most exciting growth with advancements in freeze casting, gas bubbling, and emulsion templating just to name a few. Xu asserts that, almost unexceptionally, these hierarchical porous materials have structure-enhanced performance [99]. In the world of impact resistance, hierarchical materials have been similarly successful. Estrada et al. [100] constructed hierarchical laminar organic fibrous composites with graded mineralization based on Arapaima scales and found significant improvements in energy absorption under impact. Jia et al. [101] show that using higher orders of self-similar hierarchies allowed for the improvement of stiffness, strength, and toughness simultaneously, while also confining damage to smaller length scales under dynamic loading. Using multiple structures on the same length scale gave the advantages of each, while also providing synergistic bonuses.

5.2. *Sandwich structures*

The sandwich structure is a common lightweight, impact resistant design for both high and low strain rates across many biological systems: avian beaks, bones, skulls, turtle shells, horns, pomelo peel, nuts, and wood. Two strong, stiff outer layers (faces) are separated by a softer, compliant layer (core). This arrangement accomplishes multiple goals; the hard-exterior face prevents puncture and resists repeated low strain rate impacts while the core dissipates energy and prevents cracks from bridging the two outer layers. The ultimate goal is to prevent catastrophic failure under impact. The low-velocity energy absorption mechanisms occur in the faces and the core synergistically as follows: (1) cracking, wrinkling, fracture, and delamination in the top face, (2) core buckling, (3) debonding from the faces and the core, (4) core densification and compaction, (5) shearing and cracking of the core, (6) fiber pullout in the faces, and (7) damage initiation in the bottom face [102–106]. These energy absorbing mechanisms are strongly dependent on the material properties of the faces and core (e.g., stiffness of the faces, density and degree of cross-linking in the core) and geometry (e.g., aspect ratio, face thickness to core thickness ratio, cell structuring in the core). Overall, the sandwich structure increases the amount of strain energy a material can absorb while spreading the force of the impact over a large area and arresting cracks at pore and layer interfaces. This section provides guidelines for developing tailorable impact resistant sandwich structures inspired by nature.

5.2.1. *Introducing wavy cell structure increases energy absorption*

Inspired by the wavy interface found in woodpecker beaks, Ha et al. [107] used finite element modeling to probe the effects of a wavy honeycomb wall (BHSP) compared to a conventional flat wall (CHSP) on energy absorption during impact with a velocity of 10 m/s (Fig. 8). Both BHSP and CHSP had the same core volume, wall length (9 mm), and wall height (15 mm), with varying thickness. The bioinspired wavy honeycomb wall had a wave amplitude (A) of 1 mm, wave number (n) of 2, and wavelength of 4.5 mm, and a thickness (t) of 0.1 mm. For the conventional honeycomb wall case-one (CHSP-1) the wall thickness was 0.1 mm and case-two (CHSP-2) the wall thickness was 0.132 mm.

The wavy bioinspired sandwich structure is able to withstand greater peak forces before deformation than the conventional (CHSP-1) arrangement with the same wall thickness (Fig. 8 (A-D)). However, a similar peak force was obtained for CHSP-2 having a thicker wall. The specific energy absorption (energy absorption per unit mass) is used to describe the structures' ability to dissipate energy upon impact through plastic deformation. The wavy honeycomb wall showed an increase in specific energy absorption by 125% when compared to CHSP-1 and an increase of 63.7% when compared to CHSP-2 (Fig. 8C). This is primarily due to competing deformation mechanisms. The conventional honeycomb is limited to cell-wall buckling, while the bioinspired-wavy honeycomb not only buckles, but bends and shears at the peaks and troughs of the wave allowing for an increase in plastic deformation without catastrophic failure. Additionally, the specific energy absorption can be tailored by adjusting the wave number and amplitude.

5.2.2. *Fluid-filled honeycomb increases energy absorption*

Hydration is a hallmark of biological materials and the presence of fluid has important mechanical implications for impact response. Inspired by the fluid-filled cells found in fruit peels such as the banana, Clark et al. [108] investigated the role of non-Newtonian fluid added to honeycomb structures and their ability to absorb impact energy. An impacting ram with an average kinetic energy of 0.9644 J was used for testing. With the use of a high-speed camera, the deceleration of the empty honeycomb and six layers filled with the shear-thickening fluid was 277.8 m/s^2 and 634.9 m/s^2, respectively. This corresponds to a 52.4% increase in energy absorption upon impact for the fluid-filled honeycomb structure with respect to the sample without fluid. The shear-thickening fluid stiffens upon impact and acts to redistribute the stress which reduces global damage. Investigating shear-thickening fluids in sandwich structure cores for impact response has recently been popularized. The general consensus is that their ability to absorb impact energy and suppress damage enhances the impact response of sandwich structures [109–111].

5.3. *Tubular*

The tubule architecture is defined by having hollow or fluid-filled channels organized along a similar direction. Many remarkable energy absorbent materials found in nature including bones, teeth, exoskeletons, horns, and hooves are known to harness this design strategy. Radius, volume fraction, wall thickness, orientation, material composition, and degree of reinforcement are important factors that influence mechanical response. Typical energy absorbing mechanisms for the tubule structure are buckling, bending, collapse, delaminating, vibration, and inhibiting crack propagation. Ultimately, tubules enhance impact resistance by increasing

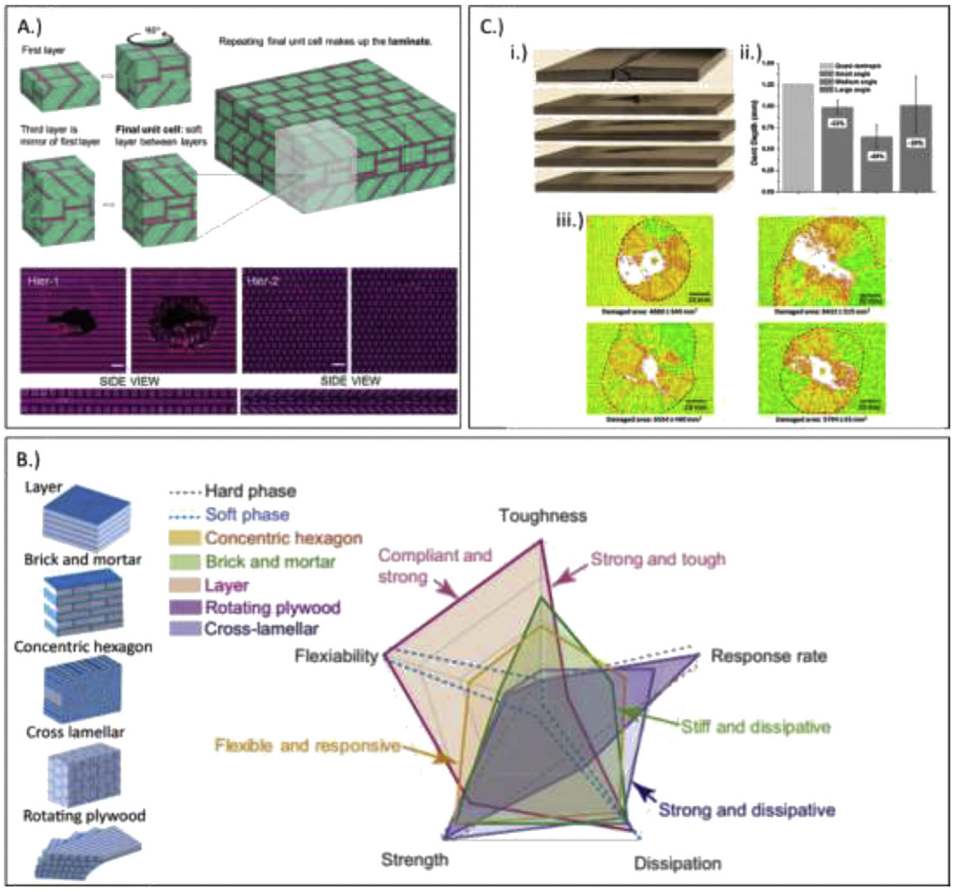

Fig. 9 – Bioinspired layered structures. A.) (Top) Visualization of 3D printed samples inspired by cross-lamellar structure of conch shell with a layer-by-layer construction of the repeating unit cell that forms the final structure. (Bottom) The single level of hierarchy and the conch-inspired designs after impact from a top and side view. Minimal damage is seen in the conch-inspired design with two levels of hierarchy [115]. B.) Comparison of properties of five different 3D printed lamellar arrangements [101]. C.) (i) Impact damage in fiber-reinforced composite samples with different layup arrangements. From top to bottom the samples are unidirectional, quasi-isotropic, small-angle helicoidal, medium-angle helicoidal, and large-angle helicoidal. (ii) Comparison of dent depth from drop tower indenter across the bottom four samples in (i). The isotropic sample was completely fractured. (iii) Image from ultrasonic C-scan indicating the extent of internal damage in the quasi-isotropic (top left), small-angle (top right), medium-angle (bottom left), and high-angle (bottom right) samples [123]. Adapted with permission [115] Copyright 2017, Wiley. Adapted with permission [101] Copyright 2018, Elsevier. Adapted with permission [123] Copyright 2014, Acta Materialia.

energy absorption via these plastic deformation mechanisms and by deflecting cracks.

5.3.1. *Tubule thickness and deformation mechanisms*

Inspired by the cuticle of the elytra beetle, Hao and Du [112] investigated the role of tubules within the thickness of the cuticle (pores) and larger hollow tubules that support the cuticle and their relative deformation mechanisms under impact with the use of numerical modeling. This can be viewed as two orders of the tubule structure where the diameter of the tubule in the cuticle is much smaller than the supporting tubule beneath (Fig. 8 (E-J)). Hao and Du performed impact tests on structures with and without tubules in the cuticle layer. The presence of tubules in cuticle helps to absorb energy upon impact. This is explained by its ability to resist catastrophic deformation. In the case without cuticle pores, the support tubule buckles and collapses. However, with the tubule in the cuticle layer, the support tubule only slightly buckles as impact energy is used to split the cuticle pore and expand the upper diameter of the support tubule (Fig. 8 (F,G)).

Additionally, Hao and Du [112] investigated the influence of the inner diameter in the support tubules on impact deformation, while the wall thickness remains constant (Fig. 8 (H-J)). For all cases, the cuticle pore remains the same size and deforms by delaminating and expanding at the base. For small diameters, the support tubule buckles in an "s" shape. The medium-diameter has an expansion with only slight buckling while the largest diameter buckles the least and has the greatest expansion. This behavior can be explained by changes in the moment of inertia and resistance to bending.

Increasing the diameter and keeping the wall thickness constant allows for an increase in strain. This suggests that larger diameters may absorb more impact energy through conversion to strain energy.

5.3.2. *Increasing tubule hierarchy increases energy absorption*

Inspired by the hierarchical organization of tendons, Tsang and Raza [113] simplified fiber bundles as hollow tubular sections to investigate the role of hierarchy on impact absorption using numerical modeling. The collision was modeled with an impact mass of 200 kg and a velocity of 20 m/s. Three orders of hierarchy were investigated where the first order is a simple hollow tube with each sequential order fitting seven hollow tubes within one larger tube (Fig. 8 (K–O)). Under impact loading, peak von Mises stress, strain, vertical displacement, contact force, and total energy all decrease with increasing hierarchy (Fig. 8 (K,L)). The peak von Mises stress occurs just below the point of contact and reduces from 485 MPa to 337 MPa–198 MPa from first- second- and third-order hierarchy, respectively (Fig. 8 (M–O)). There is reduction in total energy of 73% and 89% for the second- and third-order, respectively, when compared to the first-order hierarchy. With each increasing hierarchy there is greater surface area to better distribute the load allowing for delocalization of stress and strain.

5.4. *Layered structures*

Layered composite arrangements are a hallmark of biological materials. These are abutted layers of material that have different properties, often with the goal of creating a weak sacrificial interface between them. This sacrificial layer frequently serves to deflect cracks that propagate during impact, forcing them to take tortuous, energy-absorbent paths. This structure is found in a wide range of organisms and can be made of both mineralized and unmineralized tissues. In a review of impact resistant mammalian structures for bioinspiration, McKittrick et al. [114] determined that the microdeformation mechanics of lamellar structures such as microbuckling and delamination made them the best energy-absorbent designs. The combination of beneficial fracture dynamics and energy-absorbent deformation modes have made natural lamellar materials an exciting topic of research in the past half century. Layered structures come in a variety of different arrangements which create tortuous fracture paths and crack arresting interfaces, while also dissipating energy through delamination and buckling.

5.4.1. *Effect of additional levels of hierarchy and interface angle*

Gu et al. [115] 3D printed cross-lamellar structures inspired by the conch shell. They made two different models, one with a single level of hierarchy consisting of three stacked layers orthogonal to each other and one with an added level of hierarchy and a crossed lamellar structure with layers at a 45° angle to each other. These are shown in Fig. 9A (top). The same crack deflection patterns as noted in quasi-static testing of the conch shell were seen in the impact testing of these biomimetic samples with crack deflection at the interfaces and delocalized damage as various sections of architecture worked in concert to resist catastrophic failure. Fig. 9A (bottom) shows the effectiveness of the conch design, with minimal impactor penetration and hardly any visible damage. Gu et al. [115] also used finite element analysis to recreate impact conditions on both models. The crossed-lamellar arrangement proved to be 70% more impact resistant than the simple orthogonal geometry and 85% better than a bulk slab of the stiff phase with the same dimensions. In numerical simulations, distributed microcracking in the soft phase, which has been observed during quasi-static tests on the conch shell, was observed in the complex model, while localized damage created holes and caused catastrophic failure in the model with a single hierarchy. Gu et al. [115] calculated that cracks will deflect into the soft phase, when the interface angle is below a critical angle of 50°. This makes the 45° angle found in the conch shell optimal for deflecting cracks and preventing failure at high strain rates.

5.4.2. *Effect of layered arrangement*

Jia et al. [116] performed split Hopkinson bar testing on a range of 3D printed biological structures that mimic renowned impact resistant biological materials. These included layered, hexagonal concentric, brick and mortar, cross-lamellar, and rotating plywood structures representing the microstructure of the sea sponge, bone, nacre, conch shell, and mantis shrimp, respectively. These microstructures are visualized in Fig. 9B, along with comparative results for each. The layered structure had the best energy dissipation and critical energy (energy required to induce failure), but had a lower stiffness and response time (time needed for the impactor to complete rebound at velocities below the critical velocity). Digital image correlation was used to observe that much of this energy dissipation was the result of shear deformation between the layers. The rotating plywood and cross-lamellar structures were stiffer and more responsive than the layer section alone. However, while the cross-lamellar structure fractured at a critical energy 50% higher than the hard phase alone, the rotating plywood structure did not perform better than the hard phase. Jia et al. [116] suggested that the rotating plywood structure is effective as a crack arrester but allows easy crack initiation. This makes it effective in conjunction with other design elements that prevent cracks from initiating, where it can be used as a safeguard to prevent catastrophic failure once cracking has begun. The final two designs, brick and mortar and hexagonal concentric showed significant improvements in toughness, flexibility, and energy dissipation compared to the hard phase and stiffness, toughness, strength, and response time compared to the soft phase. Observations of these structures showed highly localized strain and microcracking throughout the material. The localized strain leads to magnified energy dissipation in the soft phase and higher stress which boosts strength and response time. The microcracking spreads damage over a larger volume, improving the overall toughness [101,116].

Ghazlan et al. [117] mimicked the polygonal brick and mortar structure of nacre to investigate the performance of a bioinspired composite panel under blast loading. Compared to a monolithic panel of equal mass, the nacre-like panel

dissipated a significant amount of energy which was attributed to crack deflection and bridging by the mortar-like bonds. In the same way, Flores-Johnson et al. [118] mimicked the staggered structure of nacre to simulate the behavior of a bioinspired composite panel under impact loading, which showed a notable reduction in the residual velocity of the impacting projectile compared to an equivalent monolithic panel. Tran et al. [119] also developed a nacre-inspired composite panel by mimicking the interfacial waviness between adjacent bricks in nacre. They observed well-distributed damage at the interface of the composite by underwater blast loading, which results in prominent energy dissipation. Ghazlan et al. [120] developed an analytical model to capture the influence of nacre's interfacial geometry on its energy absorption capacity. They employed a typical lap joint modeling approach used in structural engineering, which assumes that tension through the bricklike tablets is transferred via shear through the interface. The results indicated that the waviness of the nacreous tablets amplifies the energy absorbed by the composite whilst improving the distribution of shear forces along the interface. Miranda et al. [121] used Finite Element Modeling (FEM) to test a variety of differently-shaped armors composed of non-overlapping alumina epoxy tiles under ballistic impact. They found that hexagonally shaped tiles performed better than diamond, square, and circular tiles, providing the most uniform levels of protection, best reduction in projectile speed, and one of the smallest areas of damage. These results are unsurprising since many natural armors, like that of the armadillo and boxfish, have evolved arrangements based on hexagonal scales.

5.4.3. *Layered composites with helicoidal fiber arrangement*

Apichattrabrut et al. [122] tested helicoidally arranged carbon-fiber composites and found that they performed significantly better than unidirectional and ±45° fiber reinforced composites in both quasi-static tension and bending tests as well as impact tests. In quasi-static tests, crack propagation in the engineered twisted composite proved to be similar to those observed in similar biological materials, where cracks propagate in a helicoidal pattern that mimics the pattern of the fibers. Impact testing was performed using a vaguely bullet-shaped polycarbonate rod propelled at the samples at 55 m/s. Each layer of the ±45° composite delaminated under impact and cross cracking was observed between fibers while the projectile remained embedded in the sample once it came to a stop. In the helicoidal composite, the projectile did not penetrate the sample. Localized damage was observed on the surface and only a single layer of delamination was apparent within the composite [122]. More in-depth testing on helicoidal composites inspired by the mantis shrimp dactyl club affirmed the beneficial impact resistance of the Bouligand structure. Fig. 9C (i) shows images of five composite samples with different ply orientations after drop tower impact testing. The top sample is a unidirectional composite with all fibers aligned in the same direction and the second is a quasi-isotropic sample with fibers oriented at 0°, ±45°, and 90° to each other. The bottom three samples have helicoidally arranged fibers with angles between adjacent layers of 7.8°,16.3°, and 25.7°. The unidirectional samples failed completely after impact testing. The helicoidal samples had a smaller dent depth (ii) after impact, which was attributed to an in-plane spread of damage. This is illustrated in Fig. 9C (iii), which shows ultrasonic C-scans of the damaged composites and indicates a larger damage area in the helicoidal samples relative to the quasi-isotropic samples [123]. These results have been confirmed by other studies and some have also noted that helicoidal composites have a higher extent of delamination during impact [124]. Further experiments involving 3D printed composites, composites fabricated from prepregs, and simulations under quasi-static bending showed that the crack twisting mechanism of Bouligand structures can delay catastrophic failure despite competing failure mechanisms, such as delamination and crack branching [125].

Helicoidal nanofiber arrangements have also been tested in nanofiber film applications. Chen et al. [126] performed falling ball experiments on epoxy films without nanofibers, with orthogonally oriented nanofibers, and with electrospun nanofibers oriented in a helicoidal arrangement. The drop height necessary to fracture the helicoidally arranged fibers was four times that of the neat epoxy film and twice the height of the orthogonal nanofiber samples. As with larger samples, a zigzag fracture pattern was observed in the helicoidal samples indicating the crack was forced to follow a tortuous path. When the film was coated on a glass slide, it outperformed toughened glass films and resin films under impact.

5.5. *Gradient structures*

Often interfaces in materials are weak points that concentrate stress and lead to failure. To effectively transfer energy to a new phase of material with different mechanical properties, biological materials will often gradually change the properties of the material, rather than produce a discrete boundary [127]. This gradual change in mechanical properties is frequently referred to as a gradient structure and falls into the classification of Functionally Graded Materials (materials that change in composition, constitution, or structure continuously through its thickness). These materials have garnered significant interest for armors meant to resist impacts in the ballistic regime. Multilayer ceramic armors are commonly used for bullet proofing in military applications. These materials often delaminate as the tensile wave caused by a bullet reaches the interlayer where there is a mismatch in mechanical properties. Functionally graded ceramic armor reduces this mismatch and creates an optimal impact resistant material [128]. Long before the first ceramic bulletproof vests were being prototyped for the Vietnam War, nature was optimizing structural gradients in a host of biological materials. While interfaces can arrest cracks, they can also act as initiators where internal stresses are focused. Gradients in material properties eliminate these local concentrations and can also lead to crack tip blunting and deflection.

5.5.1. *Compositional gradients*

Graupner et al. [129] created composite samples that mimicked the compositional gradient of the coconut pericarp. They produced samples out of cellulose fiber reinforced polylactide acid (PLA), using fibers of different strengths, stiffness, and elongation at failure embedded in a PLA matrix to

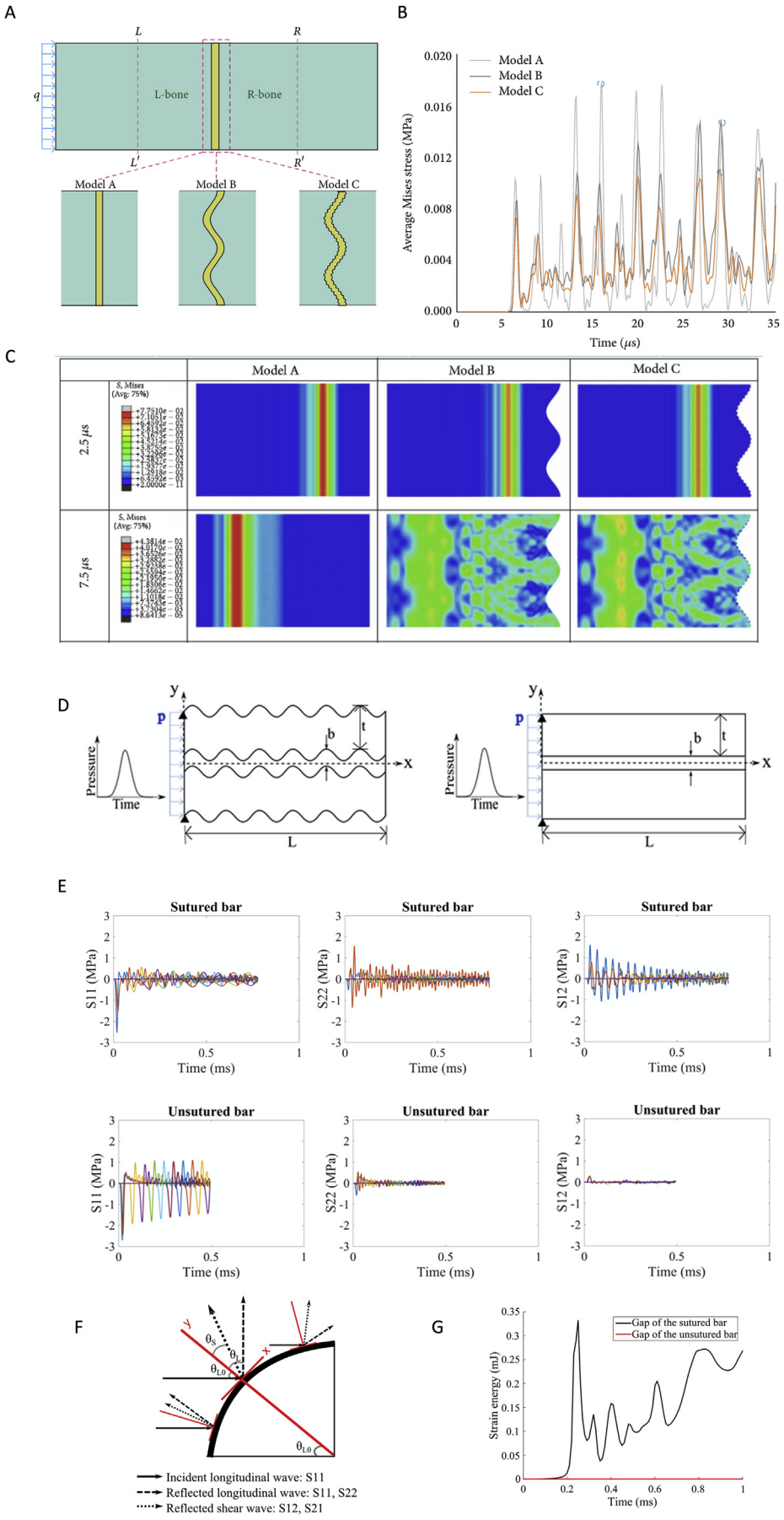
A
L
R
q
L-bone
R-bone
L′
R′
Model A
Model B
Model C
B
Model A
Model B
Model C
Average Mises stress (MPa)
Time (μs)
C
Model A
Model B
Model C
2.5 μs
7.5 μs
S, Mises
(Avg: 75%)
D
p
Pressure
Time
b
t
x
y
L
E
Sutured bar
Unsutured bar
S11 (MPa)
S22 (MPa)
S12 (MPa)
Time (ms)
F
Incident longitudinal wave: S11
Reflected longitudinal wave: S11, S22
Reflected shear wave: S12, S21
G
Gap of the sutured bar
Gap of the unsutured bar
Strain energy (mJ)
Time (ms)

recreate the steady change in mechanical properties found in the coconut. Samples with three and five layers were tested alongside reference samples to understand the effect a gradient in mechanical properties would have on the material's impact resistance. They found a threefold improvement in impact strength between the gradient structure and neat composites with the same fiber fraction, indicating that the gradient does in fact boost impact strength. Further, impact testing revealed that the five-layer composites performed significantly better than the three-layer composites, which suggests that a more gradual gradient results in better impact resistance. Graupner et al. [129] suggested that this was due to the smaller difference in properties at the interface, which decreases stress concentrations and increases the load transfer capabilities of the material.

Gradient structures improving impact resistant properties may seem to be antithetical to the improved impact resistance found in lamellar structures, which capitalize on sudden changes in material properties and significant soft–hard interfaces. However, Mirzaali et al. [130] studied the impact resistance of 3D printed materials with continuous gradients in hardness compared to materials whose hardness was a stepwise function and found that each were effective in different ways. Continuous gradients showed a higher fracture energy for cracks along the gradient direction, while stepwise functions showed better crack resistance as the hard–soft interfaces arrest crack development. Intriguingly, Mirzaali et al. [130] also found that as the transition zone between the soft and hard regions varied from 100% to 5% of the sample length nearly all fracture properties of the material increased.

5.5.2. *Porous gradients*

Bamboo and palm trunks have attracted significant attention in recent years due to their impressive energy absorption mechanisms and low density [131]. Zou et al. [132] confirmed that the gradient in vascular pores improves the impact resistance with drop tower tests before creating a bionic model that replicated the porous gradient through bamboo's cross section. This model was numerically tested and showed improved lateral impact and bending strength over models that did not contain the functional porous gradient. Chen et al. [133] 3D printed samples with a gradient in vascular pores and performed drop tower testing on the them. They discovered that the gradient increased the amount of energy that could be absorbed by the cylinders but that they also increased the peak force experienced by the structure. This occurs because the cross-sectional pores collapse and interfere with each other which allows the structure to absorb more energy, but can also prevent further deformation that is seen when there is a uniform distribution of pores throughout the material. It has also been determined that pore shape, pore size, wall thickness, rib thickness, rib angle, and a number of other parameters are intertwined with the porous gradient in making bamboo impact resistant [132–136].

5.6. *Sutures*

Suture interfaces are defined as a compliant interlocking junction that connects adjacent components allowing for regional control over strength, stiffness, and energy absorption. They are found across a diverse range of biological materials including those that are known to withstand large impact forces: human skull [137,138], woodpecker beak [139], turtle shells [62,140], boxfish plates [141], pangolin scales [26], and horse hooves [32] to name a few. The suture structure is incorporated in both mineralized (e.g., skull) and non-mineralized materials (e.g., hoof). Typically, there also exists a viscoelastic material within the gap of the suture interface, often collagen, that holds the plates together. Thus, there exists a dependence on performance with material properties such as elastic modulus. Additionally, there is a wide range of geometrical features that span across biological materials including degree of interdigitation, shape (triangular, trapezoidal, sinusoidal, etc.), and hierarchical ordering. Therefore, both the material properties and geometry of the suture structure are important in determining its ability to dissipate energy during impact. Suture structures improve impact resistance by creating a flexible joint that can dissipate energy under impact without failing, while also limiting the total deformation of the junction when the interlocking mechanism catches.

The response of suture structures to impact is widely studied with respect to human skulls due to the implications for traumatic brain injuries. This is primarily accomplished through parametric studies on material property and geometry with the use of finite element analysis and/or mechanical testing of 3D-printed prototypes. The suture structure is often simplified and reduced in complexity to isolate the design features of interest (e.g., interlocking angle, waviness, hierarchical order).

5.6.1. *Increasing suture hierarchical order effectively attenuates stress*

Zhang and Yang [142] used a sinusoidal model with two orders of hierarchy in a two-dimensional finite element model to describe how suture morphology influences stress attenuation and energy absorption under dynamic loading conditions. The first order of hierarchy is a simple sinusoidal function (model B) and the second order of hierarchy contains the pure sinusoidal function with an additional sinusoidal wave on a smaller length scale (model C) (Fig. 10 A). Analysis

Fig. 10 – Bioinspired suture designs (figure on previous page). A-C) Hierarchical suture morphology and stress attenuation. A) Describes the three different suture morphologies and loading conditions. Model A is the flat interface. Model B is the simple sinusoidal suture. Model C is the second-order, hierarchical sinusoidal suture. B) Average von Mises stress at position R–R′ for the three different morphologies. C) Illustrates the time-dependence and stress distribution among the different morphologies [142]. D-G) Stress distribution mechanism in sutured interfaces. D) Schematic of the suture and flat interface and their corresponding loading conditions. E) Stress with respect to time for suture and flat interface. F) Respective orientation of incident and reflected stress waves. G) Strain energy as a function of time in the gap of the sutured and flat bar [143]. Adapted with permission [142]. Copyright 2015, Z. Q. Zhang and J. L. Yang. Adapted with permission [143]. Copyright 2014, IOP Publishing.

was also performed on a flat interface as a control labeled as model A (Fig. 10 A). Each interface joined two neighboring bone pieces labeled L-bone and R-bone (left and right, respectively). An impulsive load, q (50 kPa), was applied on the outer surface of L-bone for 0.04 μs which represents physiological dynamic loading conditions.

The sectional stress was measured at R–R' (labeled in Fig. 10 A) and plotted in Fig. 10 B to highlight the influence of suture morphology and hierarchical order. The flat interface has the largest average von Mises stress while the second-order hierarchical suture has a significant reduction in stress (Fig. 10 B). This suggests that the higher ordered suture structure acts as a transmission barrier to better attenuate the impact stress. This agrees with stress wave theory as increasing the hierarchy effectively increases the contact area with the transmitted stress wave. The suture morphology is also important in efficiently distributing the stress uniformly across the entirety of the bone (Fig. 10 C). This is caused by scattering at the interface. The higher order hierarchy also correlated to an increase in the strain energy ratio, implying its ability to store energy during impact. Additionally, this study evaluated the effect of elastic modulus on strain energy and demonstrated that as elastic modulus of the suture increases the strain energy decreases. This indicates that stiffness can be tailored to optimize strain energy storage. This study purposefully omitted the viscoelastic response that is typically associated with the suture interface to isolate the dependence on morphology.

5.6.2. *Mechanism for stress distribution in suture interfaces*

While Zhang and Yang [142] formally described the ability of sutured interfaces to attenuate stress, there was a lack of understanding of the exact mechanisms at hand. Lee et al. [143] used a similar two-dimensional finite element analysis under dynamic loading conditions to compare how stress waves were mitigated between a sinusoidal suture interface and a flat interface. In contrast to Zhang and Yang [142], Lee et al. [143] applied a loading direction perpendicular to the interface (Fig. 10 D). They examined the damping capabilities and showed that the flat interface was able to reduce the initial pressure wave by 53% while the sutured interface had a reduction of 90%. The dominating mechanism at hand is the conversion of compressive waves (S11) to shear waves (S12) and orthogonal flexure waves (S22) due to scattering at the interface as shown in Fig. 10 E. Another attenuation mechanism was described by the viscoelastic response within the gap of the suture that allowed for strain energy storage (Fig. 10 G).

5.6.3. *Geometric influence on stress wave mitigation*

Lee et al. [143] performed a parametric study across a range of geometrical constraints including waviness, ratio of the suture height to the thickness of the bar, gap thickness, and type of boundary. The one geometric design that was shown to have the largest effect on damping was the ratio of the suture height to the bar thickness. The pressure loss was the greatest in the sample that had the largest height of the suture when the bar thickness was conserved. Interestingly, they did not see large variations with respect to waviness (wave height divided by wave period). They analyzed damping due to waviness from 0.25 to 1.5 while a higher range is seen in nature, 1 (woodpecker) and 2.4 (bison) [143].

5.6.4. *Effect of loading direction*

While the two aforementioned studies [142,143] prove that suture interfaces are superior to flat interfaces in damping and attenuating stress despite loading direction (parallel vs perpendicular), it is necessary to compare how loading direction influences the impact response. The contribution of Maloul et al. [144] demonstrates the distinction between loading direction (parallel vs perpendicular) and strain energy. Loading parallel to the suture interface resulted in the highest strain energy output. This suggests that the parallel direction is more efficient in absorbing energy. For both loading directions, the highest stresses are observed at the peaks of the sutures. While the loading conditions in nature are much more complex and difficult to predict, this study provides the basis for tailorable design for specific applications under dynamic conditions.

Overall, there are limited studies that have investigated the geometrical and material property relationship found in sutures under dynamic loading conditions, and the studies that do exist rely heavily on FEA. These few studies have shown the important role that sutures play in distributing stress and dissipating energy under high strain rates. There is clear evidence that suture geometry, elastic modulus, viscoelastic properties, and loading direction work synergistically to enhance performance under dynamic conditions.

6. Current engineered impact resistant materials

There is an increasing demand for lightweight materials and structures with high energy absorption capacity in automotive, naval, aerospace, construction, defense, personal protection, sports, and other industries. Engineered materials, such as steels and other alloys (titanium, aluminum, magnesium) and composites are being continuously developed, with performance tailored to crashworthiness, internal damping, and improved crack resistance. Also, designs often combine different classes of materials to achieve superior performance. The Chobham armor is a splendid example of a multi-component system designed to resist defeat by shaped charges, high explosive anti-tank rounds, and kinetic energy penetrators [145]. The armor is composed of ceramic tiles encased within a metal framework and bonded to a backing plate and several elastic layers. Thus, it contains ceramic, metal, polymer, and composite elements. Many other current technological applications and challenges involve similar structural and material complexity.

Body armors have been used for centuries to protect against penetration by weapons and disperse impact energy [146]. Standard features of these armors are ballistic fibers which are woven in two- or three-dimensional arrays. Fiber architectures, including their density, stiffness, and interfaces control the speed of stress waves and their dispersion [147]. Multi-layered systems absorb energy through interfaces. Shear thickening fluids have also been used to enhance

friction and dampen waves [148–150]. High-performance fibers include synthetic choices (e.g., Kevlar) or natural fibers (e.g., cotton, wool, sisal, jute, silk). Natural fibers have high energy-absorbing capacity. Their other advantages include availability, cost-effectiveness, biodegradability, and environmental safety [147]. Highly effective designs in mediating impacts are composite sandwich-like structures, as in the Chobham armor. The designs include a robust outer layer, soft-fill middle layer, and a plastic backplate. The outer sheet, usually made of ceramic, dissipates energy by brittle failure and fragmentation and deflects or damages the impactor. The core consists of a laminated composite which delaminates or a foam which deforms inelastically to absorb and dissipate energy. Metal (or composite) backing further dissipates energy by deforming plastically and containing armor and impactor fragments. Ceramic outer cores are made of alumina, boron carbide, titanium diboride, silicon carbide, and other high hardness materials [151]. Such sandwich designs are similar to a turtle shell or skull structure.

With the goal of reducing greenhouse gases and improving fuel efficiency, many have begun to investigate lightweight and sustainable energy absorbing materials. In the automotive industry, engineers are replacing steel with aluminum and magnesium alloys, composites, and foams [152]. The vital design consideration in automobiles, trains, aircraft, boats, and ships is crashworthiness and penetration resistance. The energy of the impact needs to be dissipated in a controlled manner before it enters the passenger compartment. Composite materials and plastics with synthetic and natural fibers as reinforcement are increasingly being utilized. Interest in natural fiber composites is growing due to environmental considerations and cost. Polymer-matrix composite materials are of particular interest to aerospace, automotive, naval, defense, and wind power industries also due to their high strength/stiffness to weight ratio. Composites are reinforced with fibers in various forms, such as short fibers, long fibers, and mats, with filler sizes ranging from microns to nanometers. The properties of composites depend on the properties of their matrix and fillers, filler shape and arrangement, interfacial bonding, and size of fillers. Polymer-matrix composites have excellent energy absorption characteristics due to their viscoelastic properties and various energy dissipation mechanisms. The damage mechanisms include delamination, matrix cracking, and fiber/yarn breakage. Drawbacks are that such internal damage degrades the material properties and reduces the load-carrying capacity of the structure [153]. Thus, more damage-tolerant composite materials are needed for high end and multi-use applications.

Nanocomposite materials, which are composites with nano-sized fillers, can have superior performance to traditional composites with micro-sized fillers [154]. The larger interface surface area of nanocomposites provides enhanced energy-absorbing mechanisms in the form of interfacial slipping and debonding. Also, local properties and interfacial interactions are altered since the nanofiller size is of the same order of magnitude as the molecular structure of a polymer, leading to additional toughening mechanisms [155]. Nanocomposites can reach higher strength and strain to failure than composites with micron-sized fillers [156]. Mineralized biological materials such as bone and enamel, which are examples of natural nanocomposites, similarly achieve high stiffness/strength and toughness. Nanofillers have also been added to composites to enhance matrix-fiber bonding and strengthen interfaces between plies in laminated composites, leading to composites with hierarchical structures [157–159]. Hierarchical structures are one of the key characteristics of biological materials, contributing to their robust properties.

The construction industry utilizes concrete, which is the most widely used material [160]. Concrete structures serve under conditions of frequent or occasional impact loads (wind, waves, blasts). Examples include airfield runways subjected to dynamic aircraft landing forces, buildings exposed to strong winds and earthquakes, and offshore structures, protection barriers, and dams that are subjected to waves. Conventional concrete has limited deformation and low energy-absorption capacity, which poses a challenge to the safety of these structures under impact loading conditions [161]. Thus, high-performance fiber reinforced concrete that can absorb energy has been developed. Ongoing research addresses various energy absorption components to optimize the impact resistance of concrete. For example, granulated rubber particles added to concrete improved impact resistance of concrete [162].

Synthetic cellular materials such as honeycomb-like materials made of parallel prismatic cells or closed-cell random foams are utilized in the automotive and aerospace industries for impact energy absorption. Polymeric foams, such as Styrofoam, are used for packaging. Foams are also used for thermal insulation, structural functions, buoyancy, and other applications such as filters, water repellent membranes, and antistatic shields. Foaming allows for a broader range of properties. Foams enable the production of lightweight and stiff components such as sandwich panels, portable structures, and floating devices. The low thermal conductivity of foams yields cheap thermal insulators, the low stiffness makes them desirable for cushioning, while low strengths and large compressive strains provides ideal energy absorption [163,164].

Various cellular materials' architectures are being explored, ranging from honeycomb to truss-like structures to auxetic structures with unusual properties (e.g. negative Poisson's ratio) not achievable by traditional materials. Functionally graded materials (FGM), which have spatially changing composition and structure (e.g. porosity), are being tailored for desired performance [165]. Applications include energy-absorbing structures, heat exchangers, optoelectronic devices, and medical implants for automotive, aerospace, medical, and other industries. Advancements in additive manufacturing provide freedom in their design and facilitate their production. Compared with multiphase composites, FGMs have properties that change less abruptly, which helps to minimize stress concentrations, improving the durability of load-bearing structures. Porosity graded lattices have shown excellent energy absorption characteristics, making them candidates for various technological applications, particularly for multifunctional structures and devices [166–171]. Functionally graded structures are found in many impact-resistant biological materials, including bone, articular cartilage, and hoof wall.

Impact-resistant materials and structures are desired in various technological applications. The current state-of-the-

art is addressing these pressing technological and societal needs, but it has limitations. Bioinspiration offers a multitude of ingenious ideas on designs of new, highly impact-resistant materials. Nature has masterfully created intricate architectures, but engineers have a much more extensive range of starting materials to utilize. Bioinspiration, combined with advancements in materials synthesis, manufacturing, and computational modeling (e.g., topology optimization), opens numerous exploration opportunities. These attributes make it a fertile area for new designs and material discovery.

7. Conclusions

The ultimate goal of this review is to establish a relationship between structural elements, material properties, and their ability to withstand impact and to construct guidelines for developing impact-resistant materials/systems.

Through analysis of successful impact-resistant biological systems, clear trends in structural arrangement emerge. This study has led to a classification of impact-resistant design elements in biological materials into sandwich, layered, sutured, tubular, and gradient structures. This study has also explored ubiquitous traits of biological materials that are vital factors for impact resistance including hierarchical, composite, porous, interfacial, and viscoelastic/viscoplastic characteristics.

The most common deformation mechanism among biological materials subjected to low-velocity impact is delamination at interfaces at different structural scales, where kinetic energy is converted to free surface energy. Densification and collapse of tubules or other pores to generate strain energy is another predominating mechanism. Table S1 summarizes the biological systems, their structural elements, impact energies, and deformation mechanisms reviewed here. While many biological systems have been studied under the impact, it is not easy to decouple the contributions of their individual structural elements.

The grand challenge is to develop, from the analysis of biological structures and by classifying the fundamental mechanisms of bioinspired impact-resistant designs through advanced manufacturing techniques, appropriate mechanical testing and modeling. The generation of tunable designs via geometry and material properties allows for the investigation of how these structural elements deform, absorb, and dissipate impact energy. Through the use of modeling, many of these elements are shown to avoid catastrophic failure through stress attenuation and redistribution. These bioinspired design elements, their energy-absorbing mechanisms, and tailorable designs are summarized in Table 2.

8. Future possibilities

The development of impact resistant materials remains an enterprising challenge that is strongly dependent on two fronts: (1) understanding structure–composition–property relations accompanied by a sufficient database for tailorable design and optimization and (2) use of advanced manufacturing techniques to accomplish design requirements.

Here we suggest details that are important to achieving these two facets.

- **New manufacturing techniques**
  - o New developments in additive manufacturing accounting for complex bio-inspired architectures. The needs include printing of a wider range of materials, including multiple materials, achieving sufficient resolution and printing flexibility to manufacture hierarchical and composite structures.
  - o New hybrid systems, combining more than one manufacturing technique to create new complex structures, with added flexibility.
  - o Incorporation of biological materials, which achieve such excellent properties, into synthetic components to obtain new bioinspired materials.
  - o Creation or implementation of new synthesis methods to create new materials.
- **Establishment of relationships between quasi-static and dynamic testing and material and structural responses.** While not shown here, there have been extensive studies on the quasi-static response of these biological materials with an attempt to explain what is happening dynamically. To what extent can quasi-static results be extrapolated to the dynamic regime?
- **Advancements in testing and modeling of biological and bioinspired materials under dynamic loads.** More impact testing and modeling of biological materials and bioinspired designs is needed. Our review shows that there is limited testing of various structural elements. For example, there has been very limited studies on the effects of tubules on impact resistance, even though they are important structures in horns and hooves, and they show impressive impact resistance. Another open topic is the role of interfaces in biological and bioinspired composites.
- **Investigation of the effects of multiple structural elements acting in synergy.** How does the interaction of multiple elements in one bioinspired architecture influence impact? For example, what is the effect of combined tubules and layered structures seen in the hoof and the horn?
- **Understanding of the role of self-healing and self-repair on impact-resistance of materials and structures.** Nature can repair materials if a catastrophic failure occurs, such when a bone is broken. How does such repair play a role in the impact resistance strategies of natural materials? Can regrowth be another mechanism or structural feature contributing to material response? Biological materials might allow damage to initiate regrowth. How does such process work in time and what can we learn from it and implement in future designs?
- **Understanding of the role of structural hierarchy on materials' impact resistance.** How does hierarchy of structures contribute to the impact resistance? How do the different length scales influence the impact resistance of biological materials? When designing future bioinspired, impact resistant materials, what length scale is most important: nano-, micro-, meso-, or macro-?

- **Identification of design parameters that have the highest influence on the impact resistance of materials and structures.** Which structural design characteristics have the strongest influence on the impact resistance of materials and structures? How strong can the contribution of material components be in comparison to the effects of structural designs?
- **Optimal use of materials and porosity.** How can one utilize porosity most effectively to mitigate high stresses and provide materials resistance to dynamic loads?
- **Optimal use of fluids in the designs of impact-resistant materials.** How do fluids contribute to the impact resistance at different structural scales? How could fluid properties be tailored to achieve optimal impact resistance?
- **Creation and efficient utilization of databases for structure-composition-property relations for impact-resistant materials and structures.** Machine learning is powerful tool that can be used to guide designs of impact resistant materials and structures, if sufficient data is gathered and organized.
- **Utilization of the concepts of computational materials design proposed in Materials Genome Initiative [172] to accelerate innovation and creation of the final products.** Creation of theoretical (analytical and numerical) models and make them available for the research community to facilitate and accelerate new materials designs.
- **Creation of graphical charts to guide designs of new impact-resistant materials and structures.** Ashby diagrams or similar plots have been powerful tools to guide materials selection for various applications. However, very limited charts are available on properties linked to impact resistance, such as absorption energy.
- **Architectured, bioinspired materials and structures offer nearly unlimited possibilities of combinations of structural elements, specific dimensions, and materials choices.** How can such a large parameter space be captured effectively?
- **Preliminary research has shown that increasing the levels of hierarchy leads to improved impact resistance, but is there a limit to the effectiveness of each added length scale**? What are the tradeoffs of adding geometries on more length scales and at what point do faster impacts bypass the energy absorption mechanisms of these structures?
- **Stress wave interaction within biological materials.** A handful of studies have examined impact induced stress waves within a biological material. However, further research is needed to fully understand the role that structural features play in mitigating these wave effects.

We listed above just some of the open possibilities, questions, and opportunities. The discussion here focuses on impact resistant materials, but similar thinking applies to other classes of materials. These open scientific questions show nearly endless possibilities and present exciting opportunities for the discovery and creation of new materials. Materials play an integral role in the technological advancements of our society, with impact resistance having many important applications. Impact resistant materials can be useful for high-end applications such as protection against meteorites in space, protective armors, and sports equipment to common products such as packaging. Additional considerations for designs could include sustainability and materials reuse and repair.

This review should provide an inspiration for the research community to study a broader range of biological materials and explore the full potential of the knowledge that can be gained from nature to design new engineering materials and structures.

Declaration of Competing Interest

The authors declare that they have no known competing financial interests or personal relationships that could have appeared to influence the work reported in this paper.

Acknowledgments

Professor Joanna McKittrick was a mentor to her students, an inspiration to her colleagues, and a dear friend to all who worked with her. Many of her contributions are represented in this review as she was a pioneer in impact resistant biological and bioinspired materials. Her research left an indelible mark on the scientific community and she will be sincerely missed.

We acknowledge the funding from National Science Foundation Mechanics of Materials and Structures program (Grant numbers 1926353 and 1926361).

Appendix A. Supplementary data

Supplementary data to this article can be found online at https://doi.org/10.1016/j.jmrt.2020.10.062.

REFERENCES

[1] Patek SN, Korff WL, Caldwell RL. Deadly strike mechanism of a mantis shrimp. Nature 2004;428:819–20. https://doi.org/10.1038/428819a.

[2] Kitchener A. An analysis of the forces of fighting of the blackbuck (Antilope cervicapra) and the bighorn sheep (Ovis canadensis) and the mechanical design of the horn of bovids. J Zool 1988;214:1–20. https://doi.org/10.1111/j.1469-7998.1988.tb04983.x.

[3] Haslam M, Fujii J, Espinosa S, Mayer K, Ralls K, Tinker MT, et al. Wild sea otter mussel pounding leaves archaeological traces. Sci Rep 2019;9:1–11. https://doi.org/10.1038/s41598-019-39902-y.

[4] Wang LZ, Lu S, Liu XY, Niu XF, Wang C, Ni YK, et al. Biomechanism of impact resistance in the woodpecker's head and its application. Sci China Life Sci 2013;56:715–9. https://doi.org/10.1007/s11427-013-4523-z.

[5] Parsons KJ, Spence AJ, Morgan R, Thompson JA, Wilson AM. High speed field kinematics of foot contact in elite galloping horses in training. Equine Vet J 2011;43:216–22. https://doi.org/10.1111/j.2042-3306.2010.00149.x.

[6] Currey JD. The mechanical adaptations of bones. Princeton University Press; 1984. https://doi.org/10.2307/j.ctt7zvckf.

[7] Currey JD. The design of mineralised hard tissues for their mechanical functions. J Exp Biol 1999;202:3285–94.
[8] Vincent J. Structural biomaterials. Princeton University Press; 2012. https://doi.org/10.2307/j.ctt7tbgv.
[9] Vincent JFV, Mann DL. Systematic technology transfer from biology to engineering. Philos Trans R Soc A Math Phys Eng Sci 2002;360:159–73. https://doi.org/10.1098/rsta.2001.0923.
[10] Ashby M, Wegst U. The mechanical properties of natural materials. I. Material property charts. Proc R Soc London Ser A Math Phys Sci 1995;450:123–40. https://doi.org/10.1098/rspa.1995.0075.
[11] Meyers MA, Chen PY, Lin AYM, Seki Y. Biological materials: structure and mechanical properties. Prog Mater Sci 2008;53:1–206. https://doi.org/10.1016/j.pmatsci.2007.05.002.
[12] Chen P-Y, McKittrick J, Meyers MA. Biological materials: functional adaptations and bioinspired designs. Prog Mater Sci 2012;57:1492–704. https://doi.org/10.1016/j.pmatsci.2012.03.001.
[13] Sherman VR, Yang W, Meyers MA. The materials science of collagen. J Mech Behav Biomed Mater 2015;52:22–50. https://doi.org/10.1016/j.jmbbm.2015.05.023.
[14] Yang W, Meyers MA, Ritchie RO. Structural architectures with toughening mechanisms in Nature: a review of the materials science of Type-I collagenous materials. Prog Mater Sci 2019;103:425–83. https://doi.org/10.1016/j.pmatsci.2019.01.002.
[15] Wang B, Yang W, McKittrick J, Meyers MA. Keratin: structure, mechanical properties, occurrence in biological organisms, and efforts at bioinspiration. Prog Mater Sci 2016;76:229–318.
[16] Meyers MA, Chen P-Y. Biological materials science: biological materials, bioinspired materials, and biomaterials. Cambridge University Press; 2014. https://doi.org/10.1017/CBO9780511862397.
[17] Naleway SE, Porter MM, McKittrick J, Meyers MA. Structural design elements in biological materials: application to bioinspiration. Adv Mater 2015;27:5455–76. https://doi.org/10.1002/adma.201502403.
[18] Zukas J. Impact dynamics. John Wiley & Sons; 1982.
[19] Meyers MA. Dynamic behavior of materials. John Wiley & Sons; 1994.
[20] Kulkarni SG, Gao XL, Horner SE, Zheng JQ, David NV. Ballistic helmets - their design, materials, and performance against traumatic brain injury. Compos Struct 2013;101:313–31. https://doi.org/10.1016/j.compstruct.2013.02.014.
[21] Seidel R, Thielen M, Schmitt C, Bührig-Polaczek A, Fleck C, Speck T. Fruit walls and nut shells as an inspiration for the design of bio-inspired impact-resistant hierarchically structured materials. Int J Des Nat Ecodyn 2013;8:172–9. https://doi.org/10.2495/DNE-V8-N2-172-179.
[22] Gludovatz B, Walsh F, Zimmermann EA, Naleway SE, Ritchie RO, Kruzic JJ. Multiscale structure and damage tolerance of coconut shells. J Mech Behav Biomed Mater 2017;76:76–84. https://doi.org/10.1016/j.jmbbm.2017.05.024.
[23] Matsushita AK, Gonzalez D, Wang M, Doan J, Qiao Y, Mckittrick J. Beyond density: mesostructural features of impact resistant wood. Mater Today Commun 2020;22:100697. https://doi.org/10.1016/j.mtcomm.2019.100697.
[24] Wang L, Cui Y, Qin Q, Wang H, Wang J. Helical fiber pull-out in biological materials. Acta Mech Solida Sin 2016;29:245–56. https://doi.org/10.1016/S0894-9166(16)30159-8.
[25] Huang NC, Liu XY. Debonding and fiber pull-out in reinforced composites. Theor Appl Fract Mech 1994;21:157–76. https://doi.org/10.1016/0167-8442(94)90031-0.
[26] Wang B, Yang W, Sherman VR, Meyers MA. Pangolin armor: overlapping, structure, and mechanical properties of the keratinous scales. Acta Biomater 2016;41:60–74. https://doi.org/10.1016/j.actbio.2016.05.028.
[27] Bertram JE, Gosline JM. Functional design of horse hoof keratin: the modulation of mechanical properties through hydration effects. J Exp Biol 1987;130:121–36.
[28] Kasapi MA, Gosline JM. Micromechanics of the equine hoof wall: optimizing crack control and material stiffness through modulation of the properties of keratin. J Exp Biol 1999;202:337–91.
[29] Douglas JE, Mittal C, Thomason JJ, Jofriet JC. The modulus of elasticity of equine hoof wall: implications for the mechanical function of the hoof. J Exp Biol 1996;199:1829–36.
[30] Kasapi MA, Gosline JM. Strain-rate-dependent mechanical properties of the equine hoof wall. J Exp Biol 1996;199:1133–46.
[31] Li BW, Zhao HP, Feng XQ, Guo WW, Shan SC. Experimental study on the mechanical properties of the horn sheaths from cattle. 2010. p. 479–86. https://doi.org/10.1242/jeb.035428.
[32] Huang W, Yaraghi NA, Yang W, Velazquez-Olivera A, Li Z, Ritchie RO, et al. A natural energy absorbent polymer composite: the equine hoof wall. Acta Biomater 2019;90:267–77. https://doi.org/10.1016/j.actbio.2019.04.003.
[33] Reilly JD, Cottrell DF, Martin RJ, Cuddeford D. Tubule density in equine hoof horn. Biomimetics 1996;4:23–35.
[34] Kasapi MA, Gosline JM. Design complexity and fracture control in the equine hoof wall. J Exp Biol 1997;200:1639–59.
[35] Huang W. Impact resistant and energy absorbent natural keratin materials: horns and hooves. 2018. p. 1–213.
[36] Bertram JE, Gosline JM. Fracture toughness design in horse hoof keratin. J Exp Biol 1986;125:29–47.
[37] Seki Y, Kad B, Benson D, Meyers MA. The toucan beak: structure and mechanical response. Mater Sci Eng C 2006;26:1412–20. https://doi.org/10.1016/j.msec.2005.08.025.
[38] Lee S, Novitskaya EE, Reynante B, Vasquez J, Urbaniak R, Takahashi T, et al. Impact testing of structural biological materials. Mater Sci Eng C 2011;31:730–9. https://doi.org/10.1016/j.msec.2010.10.017.
[39] Liu S, Xu S, Song J, Zhou J, Xu L, Li X, et al. Mechanical properties and failure deformation mechanisms of yak horn under quasi-static compression and dynamic impact. J Mech Behav Biomed Mater 2020:103753. https://doi.org/10.1016/j.jmbbm.2020.103753.
[40] Drake A, Haut TL, Stansloski M, Fox K, Wheatley BB, Donahue SW. Horn and horn core trabecular bone of bighorn sheep rams absorbs impact energy and reduces brain cavity accelerations during high impact ramming of the skull. Acta Biomater 2016;44:41–50. https://doi.org/10.1016/j.actbio.2016.08.019.
[41] Huang W, Zaheri A, Jung J, Espinosa HD, McKittrick J. Hierarchical structure and compressive deformation mechanisms of bighorn sheep (Ovis canadensis) horn. Acta Biomater 2017;64:1–14. https://doi.org/10.1016/j.actbio.2017.09.043.
[42] Tombolato L, Novitskaya EE, Chen P, Sheppard FA, McKittrick J. Microstructure, elastic properties and deformation mechanisms of horn keratin. Acta Biomater 2010;6:319–30. https://doi.org/10.1016/j.actbio.2009.06.033.
[43] Trim MW, Horstemeyer MF, Rhee H, El H, Williams LN, Liao J, et al. The effects of water and microstructure on the mechanical properties of bighorn sheep (Ovis canadensis) horn keratin. Acta Biomater 2011;7:1228–40. https://doi.org/10.1016/j.actbio.2010.11.024.

[44] Fratzl P, editor. Collagen: structure and mechanics. Springer; 2008.
[45] Cowin S, Doty S. Tissue mechanics. Springer; 2007.
[46] Shen ZL, Dodge MR, Kahn H, Ballarini R, Eppell SJ. Stress-strain experiments on individual collagen fibrils. Biophys J 2008;95:3956–63. https://doi.org/10.1529/biophysj.107.124602.
[47] Shen ZL, Kahn H, Ballarini R, Eppell SJ. Viscoelastic properties of isolated collagen fibrils. Biophys J 2011;100:3008–15. https://doi.org/10.1016/j.bpj.2011.04.052.
[48] Silver FH, Freeman JW, Seehra GP. Collagen self-assembly and the development of tendon mechanical properties. J Biomech 2003;36:1529–53. https://doi.org/10.1016/S0021-9290(03)00135-0.
[49] Deymier AC, An Y, Boyle JJ, Schwartz AG, Birman V, Genin GM, et al. Micro-mechanical properties of the tendon-to-bone attachment. Acta Biomater 2017;56:25–35. https://doi.org/10.1016/j.actbio.2017.01.037.
[50] Mow V, Gu W, Chen F. Structure and function of articular cartilage and meniscus. In: Mow V, Huiskes R, editors. Basic orthop. Biomech. Mechano-biology. 3rd ed. Philadelphia: Lippincott Williams & Wilkins; 2005. p. 181–258.
[51] Mow V, Proctor C, Kelly M. Biomechanics of articular cartilage. In: Nordin M, Frankel V, editors. Basic biomech. Musculoskelet. Syst. 2nd ed. Philadelphia: Lea & Febiger; 1989. p. 31–57.
[52] Mohammadi H, Mequanint K, Herzog W. Computational aspects in mechanical modeling of the articular cartilage tissue. Proc Inst Mech Eng Part H J Eng Med 2013;227:402–20. https://doi.org/10.1177/0954411912470239.
[53] Olszta MJ, Cheng X, Jee SS, Kumar R, Kim YY, Kaufman MJ, et al. Bone structure and formation: a new perspective. Mater Sci Eng Rep 2007;58:77–116. https://doi.org/10.1016/j.mser.2007.05.001.
[54] Nordin M, Frankel V. Basic biomechanics of the muscoskeletal system. 3rd ed. Lippincott Williams & Wilkins; 2001.
[55] Cowin S, editor. Bone mechanics handbook. 2nd ed. CRC Press; 2001.
[56] Novitskaya E, Chen P-Y, Hamed E, Jun L, Lubarda V, Jasiuk I, et al. Recent advances on the measurement and calculation of the elastic moduli of cortical and trabecular bone: a review. Theor Appl Mech 2011;38:209–97. https://doi.org/10.2298/tam1103209n.
[57] O'Connor DT, Elkhodary KI, Fouad Y, Greene MS, Sabet FA, Qian J, et al. Modeling orthotropic elasticity, localized plasticity and fracture in trabecular bone. Comput Mech 2016;58:423–39. https://doi.org/10.1007/s00466-016-1301-3.
[58] Johnson TPM, Socrate S, Boyce MC. A viscoelastic, viscoplastic model of cortical bone valid at low and high strain rates. Acta Biomater 2010;6:4073–80. https://doi.org/10.1016/j.actbio.2010.04.017.
[59] Solomon SE, Hendrickson JR, Hendrickson LP. The structure of the carapace and plastron of juvenile turtles, Chelonia mydas (the green turtle) and Caretta caretta (the loggerhead turtle). J Anat 1986;145:123–31.
[60] Achrai B, Wagner HD. Micro-structure and mechanical properties of the turtle carapace as a biological composite shield. Acta Biomater 2013;9:5890–902. https://doi.org/10.1016/j.actbio.2012.12.023.
[61] Rhee H, Horstemeyer MF, Hwang Y, Lim H, El Kadiri H, Trim W. A study on the structure and mechanical behavior of the Terrapene carolina carapace: a pathway to design bio-inspired synthetic composites. Mater Sci Eng C 2009;29:2333–9. https://doi.org/10.1016/j.msec.2009.06.002.
[62] Chen IH, Yang W, Meyers MA. Leatherback sea turtle shell: a tough and flexible biological design. Acta Biomater 2015;28:2–12. https://doi.org/10.1016/j.actbio.2015.09.023.
[63] Alexander SL, Rafaels K, Gunnarsson CA, Weerasooriya T. Structural analysis of the frontal and parietal bones of the human skull. J Mech Behav Biomed Mater 2019;90:689–701. https://doi.org/10.1016/j.jmbbm.2018.10.035.
[64] Wu Q, Yang C, Ohrndorf A, Christ HJ, Han J, Xiong J. Impact behaviors of human skull sandwich cellular bones: theoretical models and simulation. J Mech Behav Biomed Mater 2020;104:103669. https://doi.org/10.1016/j.jmbbm.2020.103669.
[65] Brown AD, Rafaels KA, Weerasooriya T. Microstructural and rate-dependent shear response of human skull bones. 2020. https://apps.dtic.mil/sti/pdfs/AD1093618.pdf.
[66] Yoon SH, Park S. A mechanical analysis of woodpecker drumming and its application to shock-absorbing systems. Bioinspir Biomim 2011;6(1):016003. https://doi.org/10.1088/1748-3182/6/1/016003.
[67] Wang LZ, Zhang HQ, Fan YB. Comparative study of the mechanical properties, micro-structure, and composition of the cranial and beak bones of the great spotted woodpecker and the lark bird. Sci China Life Sci 2011. https://doi.org/10.1007/s11427-011-4242-2.
[68] Wang L, Niu X, Ni Y, Xu P, Liu X, Lu S, et al. Effect of microstructure of spongy bone in different parts of woodpecker's skull on resistance to impact injury. J Nanomater 2013. https://doi.org/10.1155/2013/924564.
[69] Wu CW, Zhu ZD, Zhang W. How woodpecker avoids brain injury? J Phys Conf Ser 2015. https://doi.org/10.1088/1742-6596/628/1/012007.
[70] Lee N, Horstemeyer MF, Prabhu R, Liao J, Rhee H, Hammi Y, et al. The geometric effects of a woodpecker's hyoid apparatus for stress wave mitigation. Bioinspir Biomim 2016;11(6). https://doi.org/10.1088/1748-3190/11/6/066004.
[71] Zhou P, Kong XQ, Wu CW, Chen Z. The novel mechanical property of tongue of a woodpecker. J Bionic Eng 2009;6(3). https://doi.org/10.1016/S1672-6529(08)60126-2.
[72] Launey ME, Chen P, Mckittrick J, Ritchie RO. Mechanistic aspects of the fracture toughness of elk antler bone. Acta Biomater 2010;6:1505–14. https://doi.org/10.1016/j.actbio.2009.11.026.
[73] Kamat S, Kessler H, Ballarini R, Nassirou M, Heuer AH. Fracture mechanisms of the Strombus gigas conch shell: II-micromechanics analyses of multiple cracking and large-scale crack bridging. Acta Mater 2004;52:2395–406. https://doi.org/10.1016/j.actamat.2004.01.030.
[74] Kuhn-Spearing LT, Kessler H, Chateau E, Ballarini R, Heuer AH, Spearing SM. Fracture mechanisms of the Strombus gigas conch shell: implications for the design of brittle laminates. J Mater Sci 1996;31:6583–94. https://doi.org/10.1007/BF00356266.
[75] Li H, Shen J, Wei Q, Li X. Dynamic self-strengthening of a bio-nanostructured armor — conch shell. Mater Sci Eng C 2019;103. https://doi.org/10.1016/j.msec.2019.109820.
[76] Bouligand Y. Twisted fibrous arrangements in biological materials and cholesteric mesophases. Tissue Cell 1971;4:189–217.
[77] Weaver JC, Milliron GW, Miserez A, Evans-Lutterodt K, Herrera S, Gallana I, et al. The stomatopod dactyl club: a formidable damage-tolerant biological hammer. Science 2012;336(80):1275–80. https://doi.org/10.1126/science.1218764.
[78] Song B, Lu WY, Syn CJ, Chen W. The effects of strain rate, density, and temperature on the mechanical properties of polymethylene diisocyanate (PMDI)-based rigid polyurethane foams during compression. J Mater Sci 2009. https://doi.org/10.1007/s10853-008-3105-0.
[79] McElhaney JH. Dynamic response of bone and muscle tissue. J Appl Physiol 1966. https://doi.org/10.1152/jappl.1966.21.4.1231.

[80] Kulin RM, Chen PY, Jiang F, Vecchio KS. A study of the dynamic compressive behavior of Elk antler. Mater Sci Eng C 2011;31:1030–41. https://doi.org/10.1016/j.msec.2011.03.002.
[81] Neumann M, Herter J, Droste BO, Hartwig S. Compressive behaviour of axially loaded spruce wood under large deformations at different strain rates. Eur J Wood Wood Prod 2011;69:345–57. https://doi.org/10.1007/s00107-010-0442-x.
[82] Brodt M, Lakes RS. Composite materials which exhibit high stiffness and high viscoelastic damping. J Compos Mater 1995. https://doi.org/10.1177/002199839502901402.
[83] Zhu ZD, Ma GJ, Wu CW, Chen Z. Numerical study of the impact response of woodpecker's head. AIP Adv 2012;2(4):042173. https://doi.org/10.1063/1.4770305.
[84] Edelsten L, Jeffrey JE, Burgin LV, Aspden RM. Viscoelastic deformation of articular cartilage during impact loading. Soft Matter 2010. https://doi.org/10.1039/c0sm00097c.
[85] Thielen M, Speck T, Seidel R. Viscoelasticity and compaction behaviour of the foam-like pomelo (Citrus maxima) peel. J Mater Sci 2013. https://doi.org/10.1007/s10853-013-7137-8.
[86] Ahmadi E, Barikloo H, Kashfi M. Viscoelastic finite element analysis of the dynamic behavior of apple under impact loading with regard to its different layers. Comput Electron Agric 2016;121:1–11. https://doi.org/10.1016/j.compag.2015.11.017.
[87] Ranganathan N, Oksman K, Nayak S, Sain M. Impact toughness, viscoelastic behavior, and morphology of polypropylene-jute-viscose hybrid composites. J Appl Polym Sci 2015;133(7):42981. https://doi.org/10.1002/app.42981.
[88] Harrigan JJ, Ahonsi B, Palamidi E, Reid SR. Experimental and numerical investigations on the use of polymer Hopkinson pressure bars Author for correspondence. Phil Trans R Soc 2014;372:20130201. 3023rd ed.
[89] Chen W, Zhang B, Forrestal MJ. A split Hopkinson bar technique for low-impedance materials. Exp Mech 1999;39:81–5.
[90] Siviour CR, Jordan JL. High strain rate mechanics of polymers: a review. J Dyn Behav Mater 2016;2:15–32. https://doi.org/10.1007/s40870-016-0052-8.
[91] González-Albuixech VF, Rodríguez-Millán M, Ito T, Loya JA, Miguélez MH. Numerical analysis for design of bioinspired ceramic modular armors for ballistic protections. Int J Damage Mech 2019;28:815–37. https://doi.org/10.1177/1056789518795203.
[92] Duro-Royo J, Zolotovsky K, Mogas-Soldevila L, Varshney S, Oxman N, Boyce M, et al. MetaMesh: a hierarchical computational model for design and fabrication of biomimetic armor surfaces. Comput Des 2014;60:14–27. https://doi.org/10.1016/j.cad.2014.05.005.
[93] Signetti S, Pugno NM. Modeling and simulation of bio-inspired nanoarmors. In: Schmauder S, Chen C-S, Chawla KK, Chawla N, Chen W, Kagawa Y, editors. Handb. Mech. Mater. Singapore: Springer Singapore; 2018. p. 1–29. https://doi.org/10.1007/978-981-10-6855-3_15-2.
[94] Abir MR, Tay TE, Lee HP. On the improved ballistic performance of bio-inspired composites. Composer Part A Appl Sci Manuf 2019;123:59–70. https://doi.org/10.1016/j.compositesa.2019.04.021.
[95] du Plessis A, Broeckhoven C, Yadroitsava I, Yadroitsev I, Hands CH, Kunju R, et al. Beautiful and functional: a review of biomimetic design in additive manufacturing. Addit Manuf 2019;27:408–27. https://doi.org/10.1016/j.addma.2019.03.033.
[96] Velasco-Hogan A, Xu J, Meyers MA. Additive manufacturing as a method to design and optimize bioinspired structures. Adv Mater 2018;30:1800940. https://doi.org/10.1002/adma.201800940.
[97] Studart A. Additive manufacturing of biologically-inspired materials. Chem Soc Rev 2016;45:359–76.
[98] Connors M, Yang T, Hosny A, Deng Z, Yazdandoost F, Massaadi H, et al. Bioinspired design of flexible armor based on chiton scales. Nat Commun 2019;10:1–13. https://doi.org/10.1038/s41467-019-13215-0.
[99] Xu Y. Hierarchical materials. Mod Inorg Synth Chem Second Ed 2017:545–74. https://doi.org/10.1016/B978-0-444-63591-4.00019-7.
[100] Estrada S, Munera J, Hernandez J, Arroyave M, Arola D, Ossa A. Bioinspired hierarchical impact tolerant materials. Bioinspir Biomim 2020;15:046009.
[101] Jia Z, Yu Y, Hou S, Wang L. Biomimetic architected materials with improved dynamic performance. J Mech Phys Solid 2018;125:178–97. https://doi.org/10.1016/j.jmps.2018.12.015.
[102] Chai GB, Zhu S. A review of low-velocity impact on sandwich structures. Proc Inst Mech Eng Part L J Mater Des Appl 2011;225:207–30. https://doi.org/10.1177/1464420711409985.
[103] Abrate S. Localized impact on sandwich structures with laminated facings. Appl Mech Rev 1997;50:69–82. https://doi.org/10.1115/1.3101689.
[104] Dear JP, Lee H, Brown SA. Impact damage processes in composite sheet and sandwich honeycomb materials. Int J Impact Eng 2005;32:130–54. https://doi.org/10.1016/j.ijimpeng.2005.02.005.
[105] Schubel PM, Luo JJ, Daniel IM. Impact and post impact behavior of composite sandwich panels. Composer Part A Appl Sci Manuf 2007;38:1051–7. https://doi.org/10.1016/j.compositesa.2006.06.022.
[106] Raju KS, Smith BL, Tomblin JS, Liew KH, Guarddon JC. Impact damage resistance and tolerance of honeycomb core sandwich panels. J Compos Mater 2008;42:385–412. https://doi.org/10.1177/0021998307088596.
[107] Ha NS, Lu G, Xiang X. Energy absorption of a bio-inspired honeycomb sandwich panel. J Mater Sci 2019;54:6286–300. https://doi.org/10.1007/s10853-018-3163-x.
[108] Clark J, Jenson S, Schultz J, Hoffman J, Takak S, Ali M, et al. Study of impact properties of a fluid-filled honeycomb structure. ASME Int Mech Eng Congr Expo Proc 2013;9:2–7. https://doi.org/10.1115/IMECE2013-62113.
[109] Caglayan C, Osken I, Ataalp A, Turkmen HS, Cebeci H. Impact response of shear thickening fluid filled polyurethane foam core sandwich composites. Compos Struct 2020;243:112171. https://doi.org/10.1016/j.compstruct.2020.112171.
[110] Fu K, Wang H, Chang L, Foley M, Friedrich K, Ye L. Low-velocity impact behaviour of a shear thickening fluid (STF) and STF-filled sandwich composite panels. Compos Sci Technol 2018;165:74–83. https://doi.org/10.1016/j.compscitech.2018.06.013.
[111] Warren J, Kota KR, Westberg SM, Lacy T, Kundu S, Toghiani H, et al. Hypervelocity impacts of shear thickening fluid imbibed metallic foam core sandwich panels. In: 30th technical conference of American society of composites 2015; 2015.
[112] Hao P, Du J. Mechanical properties of bio-mimetic energy-absorbing materials under impact loading. J Mater Sci 2018;53:3189–97. https://doi.org/10.1007/s10853-017-1798-7.
[113] Tsang HH, Raza S. Impact energy absorption of bio-inspired tubular sections with structural hierarchy. Compos Struct 2018;195:199–210. https://doi.org/10.1016/j.compstruct.2018.04.057.
[114] McKittrick J, Chen PY, Tombolato L, Novitskaya EE, Trim MW, Hirata GA, et al. Energy absorbent natural materials and bioinspired design strategies: a review. Mater

Sci Eng C 2010;30:331–42. https://doi.org/10.1016/j.msec.2010.01.011.
[115] Gu GX, Takaffoli M, Buehler MJ. Hierarchically enhanced impact resistance of bioinspired composites. Adv Mater 2017;29:1–7. https://doi.org/10.1002/adma.201700060.
[116] Jia Z, Yu Y, Wang L. Learning from nature: use material architecture to break the performance tradeoffs. Mater Des 2019;168:107650. https://doi.org/10.1016/j.matdes.2019.107650.
[117] Ghazlan A, Ngo TD, Tran P. Three-dimensional Voronoi model of a nacre-mimetic composite structure under impulsive loading. Compos Struct 2016;153:278–96. https://doi.org/10.1016/j.compstruct.2016.06.020.
[118] Flores-Johnson EA, Shen L, Guiamatsia I, Nguyen GD. Numerical investigation of the impact behaviour of bioinspired nacre-like aluminium composite plates. Compos Sci Technol 2014;96:13–22. https://doi.org/10.1016/j.compscitech.2014.03.001.
[119] Tran P, Ngo TD, Mendis P. Bio-inspired composite structures subjected to underwater impulsive loading. Comput Mater Sci 2014;82:134–9. https://doi.org/10.1016/j.commatsci.2013.09.033.
[120] Ghazlan A, Ngo TD, Tran P. Influence of interfacial geometry on the energy absorption capacity and load sharing mechanisms of nacreous composite shells. Compos Struct 2015;132:299–309. https://doi.org/10.1016/j.compstruct.2015.05.045.
[121] Miranda P, Pajares A, Meyers MA. Bioinspired composite segmented armour : numerical simulations. Integr Med Res 2018;8:1274–87. https://doi.org/10.1016/j.jmrt.2018.09.007.
[122] Apichattrabrut T, Ravi-Chandar K. Helicoidal composites. Mech Adv Mater Struct 2006;13:61–76. https://doi.org/10.1080/15376490500343808.
[123] Grunenfelder LK, Suksangpanya N, Salinas C, Milliron G, Yaraghi N, Herrera S, et al. Bio-inspired impact-resistant composites. Acta Biomater 2014;10:3997–4008. https://doi.org/10.1016/j.actbio.2014.03.022.
[124] Ginzburg D, Pinto F, Iervolino O, Meo M. Damage tolerance of bio-inspired helicoidal composites under low velocity impact. Compos Struct 2017;161:187–203. https://doi.org/10.1016/j.compstruct.2016.10.097.
[125] Suksangpanya N, Yaraghi NA, Pipes RB, Kisailus D, Zavattieri P. Crack twisting and toughening strategies in Bouligand architectures. Int J Solid Struct 2018;150:83–106. https://doi.org/10.1016/j.ijsolstr.2018.06.004.
[126] Chen R, Liu J, Yang C, Weitz DA, He H, Li D, et al. Transparent impact-resistant composite films with bioinspired hierarchical structure. ACS Appl Mater Interfaces 2019;11:23616–22. https://doi.org/10.1021/acsami.9b06500.
[127] Liu Z, Meyers MA, Zhang Z, Ritchie RO. Progress in Materials Science Functional gradients and heterogeneities in biological materials : design principles , functions , and bioinspired applications. Prog Mater Sci 2017;88:467–98. https://doi.org/10.1016/j.pmatsci.2017.04.013.
[128] Huang CY, Chen YL. Design and impact resistant analysis of functionally graded Al2O3-ZrO2 ceramic composite. Mater Des 2016;91:294–305. https://doi.org/10.1016/j.matdes.2015.11.091.
[129] Graupner N, Labonte D, Humburg H, Buzkan T, Dörgens A, Kelterer W, et al. Functional gradients in the pericarp of the green coconut inspire asymmetric fibre-composites with improved impact strength, and preserved flexural and tensile properties. Bioinspir Biomim 2017;12(2):026009. https://doi.org/10.1088/1748-3190/aa5262.
[130] Mirzaali MJ, Herranz A, Nava D, Gunashekar D. Fracture behavior of bio-inspired functionally graded soft – hard composites made by multi-material 3D printing : the case of colinear cracks. Materials 2019;12(17):2735. https://doi.org/10.3390/ma12172735.
[131] Ha NS, Lu G. A review of recent research on bio-inspired structures and materials for energy absorption applications. Compos B Eng 2020;181:107496. https://doi.org/10.1016/j.compositesb.2019.107496.
[132] Zou M, Xu S, Wei C, Wang H, Liu Z. A bionic method for the crashworthiness design of thin-walled structures inspired by bamboo. Thin-Walled Struct 2016;101:222–30. https://doi.org/10.1016/j.tws.2015.12.023.
[133] Chen BC, Zou M, Liu GM, Song JF, Wang HX. Experimental study on energy absorption of bionic tubes inspired by bamboo structures under axial crushing. Int J Impact Eng 2018;115:48–57. https://doi.org/10.1016/j.ijimpeng.2018.01.005.
[134] Song JF, Xu SC, Wang HX, Wu XQ, Zou M. Bionic design and multi-objective optimization for variable wall thickness tube inspired bamboo structures. Thin-Walled Struct 2018;125:76–88. https://doi.org/10.1016/j.tws.2018.01.010.
[135] Hu D, Wang Y, Song B, Dang L, Zhang Z. Energy-absorption characteristics of a bionic honeycomb tubular nested structure inspired by bamboo under axial crushing. Compos B Eng 2019;162:21–32. https://doi.org/10.1016/j.compositesb.2018.10.095.
[136] Fu J, Liu Q, Liufu K, Deng Y, Fang J, Li Q. Design of bionic-bamboo thin-walled structures for energy absorption. Thin-Walled Struct 2019;135:400–13. https://doi.org/10.1016/j.tws.2018.10.003.
[137] Sun Z, Lee E, Herring SW. Cranial sutures and bones: growth and fusion in relation to masticatory strain. Anat Rec 2004;276A:150–61. https://doi.org/10.1002/ar.a.20002.
[138] Jaslow CR. Mechanical properties of cranial sutures. J Biomech 1990;20:1808–13. https://doi.org/10.1016/0021-9290(90)90059-C.
[139] Lee N, Horstemeyer MF, Rhee H, Nabors B, Liao J, Williams LN. Hierarchical multiscale structure–property relationships of the red-bellied woodpecker Beak. J R Soc Interface 2014;11(96):20140274. https://doi.org/10.1098/rsif.2014.0274.
[140] Achrai B, Daniel Wagner H. The red-eared slider turtle carapace under fatigue loading: the effect of rib-suture arrangement. Mater Sci Eng C 2015;53:128–33. https://doi.org/10.1016/j.msec.2015.04.040.
[141] Yang W, Naleway SE, Porter MM, Meyers MA, McKittrick J. The armored carapace of the boxfish. Acta Biomater 2015;23:1–10. https://doi.org/10.1016/j.actbio.2015.05.024.
[142] Zhang ZQ, Yang JL. Biomechanical dynamics of cranial sutures during simulated impulsive loading. Appl Bionics Biomechanics 2015;2015:596843. https://doi.org/10.1155/2015/596843.
[143] Lee N, Williams LN, Mun S, Rhee H, Prabhu R, Bhattarai KR, et al. Stress wave mitigation at suture interfaces. Biomed Phys Eng Express 2017;3(3). https://doi.org/10.1088/2057-1976/aa777e.
[144] Maloul A, Fialkov J, Wagner D, Whyne CM. Characterization of craniofacial sutures using the finite element method. J Biomech 2014;47(1):245–52. https://doi.org/10.1016/j.jbiomech.2013.09.009.
[145] Mahmud A. The impact of armor on the design, utilization and survivability of ground vehicles: the history of armor development and use. Naval Postgraduate School; 2003.
[146] David NV, Gao XL, Zheng JQ. Ballistic resistant body armor: contemporary and prospective materials and related protection mechanisms. Appl Mech Rev 2009;62:1–20. https://doi.org/10.1115/1.3124644.
[147] Abtew MA, Boussu F, Bruniaux P, Loghin C, Cristian I. Ballistic impact mechanisms – a review on textiles and fibre-reinforced composites impact responses. Compos

Struct 2019;223:110966. https://doi.org/10.1016/j.compstruct.2019.110966.
[148] Qin J, Guo B, Zhang L, Wang T, Zhang G, Shi X. Soft armor materials constructed with Kevlar fabric and a novel shear thickening fluid. Compos B Eng 2020;183:107686. https://doi.org/10.1016/j.compositesb.2019.107686.
[149] Laha A, Majumdar A. Interactive effects of p-aramid fabric structure and shear thickening fluid on impact resistance performance of soft armor materials. Mater Des 2016;89:286–93. https://doi.org/10.1016/j.matdes.2015.09.077.
[150] Ding J, Tracey P, Li W, Peng G, Whitten PG, Wallace GG. Review on shear thickening fluids and applications. Text Light Ind Sci Technol 2013;2:161–73.
[151] Grogan J, Tekalur SA, Shukla A, Bogdanovich A, Coffelt RA. Ballistic resistance of 2D and 3D woven sandwich composites. J Sandw Struct Mater 2007;9:283–302. https://doi.org/10.1177/1099636207067133.
[152] Ghassemieh E. Materials in automotive application, state of the art and prospects. New Trends Dev Automot Ind 2011. https://doi.org/10.5772/13286.
[153] Hyer MW. Stress analysis of fiber-reinforced composite materials. WCB/McGraw-Hill; 1998.
[154] Sun L, Gibson RF, Gordaninejad F, Suhr J. Energy absorption capability of nanocomposites: a review. Compos Sci Technol 2009;69:2392–409. https://doi.org/10.1016/j.compscitech.2009.06.020.
[155] Fu S, Sun Z, Huang P, Li Y, Hu N. Some basic aspects of polymer nanocomposites: a critical review. Nano Mater Sci 2019;1:2–30. https://doi.org/10.1016/j.nanoms.2019.02.006.
[156] Dasari A, Yu ZZ, Yang M, Zhang QX, Xie XL, Mai YW. Micro- and nano-scale deformation behavior of nylon 66-based binary and ternary nanocomposites. Compos Sci Technol 2006;66:3097–114. https://doi.org/10.1016/j.compscitech.2005.03.020.
[157] Mourad AHI, Zaaroura N. Impact of nanofillers incorporation on laminated nanocomposites performance. J Mater Eng Perform 2018;27:4453–61. https://doi.org/10.1007/s11665-018-3523-3.
[158] Mourad AHI, Idrisi AH, Zaaroura N, Sherif MM, Fouad H. Damage assessment of nanofiller-reinforced woven kevlar KM2plus/Epoxy resin laminated composites. Polym Test 2020;86:106501. https://doi.org/10.1016/j.polymertesting.2020.106501.
[159] Bisht A, Dasgupta K, Lahiri D. Investigating the role of 3D network of carbon nanofillers in improving the mechanical properties of carbon fiber epoxy laminated composite. Composer Part A Appl Sci Manuf 2019;126:105601. https://doi.org/10.1016/j.compositesa.2019.105601.
[160] Gagg CR. Cement and concrete as an engineering material: an historic appraisal and case study analysis. Eng Fail Anal 2014;40:114–40. https://doi.org/10.1016/j.engfailanal.2014.02.004.
[161] Hao H, Hao Y, Li J, Chen W. Review of the current practices in blast-resistant analysis and design of concrete structures. Adv Struct Eng 2016;19:1193–223. https://doi.org/10.1177/1369433216656430.
[162] Li LJ, Tu GR, Lan C, Liu F. Mechanical characterization of waste-rubber-modified recycled-aggregate concrete. J Clean Prod 2016;124:325–38. https://doi.org/10.1016/j.jclepro.2016.03.003.
[163] Stevenson P, editor. Foam engineering: fundamentals and applications. Wiley Online Books; 2012. https://doi.org/10.1002/9781119954620.fmatter.
[164] Exerowa D, Kruglyakov PM, editors. Foam and foam films: theory, experiment, application, vol. 5. Elsevier; 1998. https://doi.org/10.1016/S1383-7303(13)60003-4.
[165] Xu F, Zhang X, Zhang H. A review on functionally graded structures and materials for energy absorption. Eng Struct 2018;171:309–25. https://doi.org/10.1016/j.engstruct.2018.05.094.
[166] Toudehdehghan A, Lim JW, Foo KE, Ma'Arof MIN, Mathews J. A brief review of functionally graded materials. MATEC Web Conf 2017;131:1–6. https://doi.org/10.1051/matecconf/201713103010.
[167] Sarathchandra DT, Kanmani Subbu S, Venkaiah N. Functionally graded materials and processing techniques: an art of review. Mater Today Proc 2018;5:21328–34. https://doi.org/10.1016/j.matpr.2018.06.536.
[168] Bohidar SK, Sharma R, Mishra PR. Functionally graded materials: a critical review. Int J Res 2014;1:289–301.
[169] Singh R, Bhavar V, Kattire P, Thakare S, Patil S, Singh RKP. A review on functionally gradient materials (FGMs) and their applications. IOP Conf Ser Mater Sci Eng 2017;229. https://doi.org/10.1088/1757-899X/229/1/012021.
[170] Zhang C, Chen F, Huang Z, Jia M, Chen G, Ye Y, et al. Additive manufacturing of functionally graded materials: a review. Mater Sci Eng 2019;764:138209. https://doi.org/10.1016/j.msea.2019.138209.
[171] Choy SY, Sun CN, Leong KF, Wei J. Compressive properties of functionally graded lattice structures manufactured by selective laser melting. Mater Des 2017;131:112–20. https://doi.org/10.1016/j.matdes.2017.06.006.
[172] Materials genome initiative for global competitiveness. 2011. Washington, D.C. https://www.mgi.gov/.
[173] Fessel G, Snedeker JG. Evidence against proteoglycan mediated collagen fibril load transmission and dynamic viscoelasticity in tendon. Matrix Biol 2009;28:503–10. https://doi.org/10.1016/j.matbio.2009.08.002.
[174] Handl M, Držík M, Cerulli G, Povýšil C, Chlpík J, Varga F, et al. Reconstruction of the anterior cruciate ligament: dynamic strain evaluation of the graft. Knee Surg Sports Traumatol Arthrosc 2007;15:233–41. https://doi.org/10.1007/s00167-006-0175-x.
[175] Paulos LE, Patrick W. Impact biomechanics of lateral knee bracing the anterior cruciate ligament. Am J Sports Medin 1991;19(4):337–42. https://doi.org/10.1177/036354659101900403.
[176] Burgin LV, Aspden RM. Impact testing to determine the mechanical properties of articular cartilage in isolation and on bone. J Mater Sci Mater Med 2008;19:703–11. https://doi.org/10.1007/s10856-007-3187-2.
[177] Kaleem B, Maier F, Drissi H, Pierce DM. Low-energy impact of human cartilage: predictors for microcracking the network of collagen. Osteoarthritis Cartilage 2017;25(4):544–53. https://doi.org/10.1016/j.joca.2016.11.009.
[178] Zhai X, Gao J, Nie Y, Guo Z, Kedir N, Claus B, et al. Real-time visualization of dynamic fractures in porcine bones and the loading-rate effect on their fracture toughness. J Mech Phys Solid 2019;131:358–71. https://doi.org/10.1016/j.jmps.2019.07.010.
[179] Zhang W, Wu C, Zhang C, Chen Z. Microstructure and mechanical property of turtle shell. Theor Appl Mech Lett 2012;2:014009. https://doi.org/10.1063/2.1201409.
[180] Yoganandan N, Pintar FA, Sances A, Walsh PR, Ewing CL, Thomas DJ, et al. Biomechanics of skull fracture. J Neurotrauma 1995;12:659–68. https://doi.org/10.1089/neu.1995.12.659.
[181] Wang RZ, Wen HB, Cui FZ, Zhang HB, Li HD. Observations of damage morphologies in nacre during deformation and fracture. J Mater Sci 1995;30:2299–304. https://doi.org/10.1007/BF01184577.
[182] Lin A, Meyers MA. Growth and structure in abalone shell. Mater Sci Eng 2005;390:27–41. https://doi.org/10.1016/j.msea.2004.06.072.